Basic mechanisms of RNA interference and the brain water channel Aquaporin-4

Svein Erik Emblem Moe

PhD Thesis

Institute of Basic Medical Sciences
Faculty of Medicine

University of Oslo

2017

© Svein Erik Emblem Moe, 2017

Series of dissertations submitted to the
Faculty of Medicine, University of Oslo

ISBN 978-82-8377-062-9

All rights reserved. No part of this publication may be
reproduced or transmitted, in any form or by any means, without permission.

Cover: Hanne Baadsgaard Utigard.
Print production: Reprosentralen, University of Oslo.

Acknowledgements

Doing science mentored by Torgeir Holen has been an interesting journey. His alternative pedagogic skills were useful for teaching a fresh medical student the craftsmanship of molecular biology. Starting out with easy "monkey-see, monkey do"-experiments in the lab and ending it with peer-reviewed publications was not expected when I applied a summer job back in 2004. We have had a lot of fun together all these years.

This project is indeed a team effort. It would never have been completed without the hard work of key players of "Team Moe"; Jan Gunnar Sørbø, Line Strand, Tom Tallak Solbu, Marianne Vaadal and Torgeir. Thank you for the hours we spent together in the laboratory.

Combining a surgical career within otorhinolaryngology and finishing this thesis has proven to be more time-consuming than expected, as illustrated by the years passed between finishing medical school and delivering this thesis. I would like to give my appreciation to my wife for supporting me throughout this entire process. This whole project would definitively have stranded without your encouragement.

I would also give my acknowledgement to professor Ole Petter Ottersen and all the members of Laboratory for Molecular Neuroscience, Department of Anatomy within Institute of Basic Medical Sciences. The Medical Student Research Programme at University of Oslo receives my gratitude for giving me the opportunity to do science while studying medicine. Thanks to FUGE for a grant to continue my scientific work through medical school. And I express my gratitude to Professor John Rash and colleagues at Colorado State University for their hospitality during my summer research there in 2008.

I would give my appreciation to professor Christian Drevon and Torgeir Holen for constructive feedback during the writing process.

Finally, a huge gratitude to my family for the love and support all my life.

Svein Erik Emblem Moe
Haugesund, February 2017

Table of contents

Abbreviations

ADH	anti-diuretic hormone, vasopressin
Ago-2	argonaute protein 2
ApoB	Apolipoprotein B
AQP4	Aquaporin-4
BLAST	Basic Local Alignment Search Tool
BN-PAGE	Blue Native PAGE
cAMP	cyclic adenosine monophosphate
cDNA	complementary DNA
cRNA	complementary RNA
CDS	Coding DNA sequence
CHIP28	Channel-forming Integral Protein of 28 kDa
CHO	Chinese Hamster Ovary
C. Elegans	Caenorhabditis elegans, roundworm
CMV	Cytomegalovirus
CSF	cerebrospinal fluid
DM1	dystrophia myotonica 1
DNA	Deoxyribonucleic Acid
dsRNA	double stranded RNA
ECS	extracellular space
et al.	et alii (lat.), and others
Fen1	Flap endonuclease 1
GAPDH	Glyceraldehyde 3-phosphate dehydrogenase
GFAP	Glial fibrillary acidic protein
GFP	Green fluorescent protein
HD	Huntington's disease
HSV	Herpes simplex virus
IgG	immunoglobulin G
IMP	intramembrane particles
ISF	interstitial fluid
KO	gene knockout
Kir4.1	inwardly rectifier-type potassium channel
L cell	intestinal enteroendocrine cell
LDL	low-density lipoproteins
MIP	Major Intrinsic Protein, AQP0
miRNA	microRNA
mRNA	messenger RNA
MIWC	Mercury Insensitive Water Channel, AQP4
MS	multiple sclerosis
NDI	nephrogenic diabetes insipidus
NMO	neuromyelitis optica
nt	nucleotide
OAP	orthogonal arrays of particles, square arrays
PACT	Protein activator of PKR
PAGE	Polyacrylamide gel electrophoresis
PAZ	Piwi-Argonaute-Zwille, subdomain
piRNA	PIWI-interacting RNA
PIWI	P-element Induced WImpy testis
PCR	Polymerase chain reaction
PCSK9	Proprotein convertase subtilisin/kexin type 9
PKA	protein kinase A
polyQ	polyglutamine triplet repeat
PTGS	post-trancriptional gene silencing
RACE	rapid amplification of cDNA ends
RISC	RNA-induced silencing complex
RNA	ribonucleic acid
RNAi	RNA interference
RT-PCR	reverse transcriptase PCR
SDS	sodium dodecyl sulfate
shRNA	short hairpin RNA
siRNA	small (or short) interfering RNA
TNR	trinucleotide repeat
TRPB	TAR RNA-binding protein
unc-22	uncoordinated protein 22
UV	ultraviolet
V2	Vasopressin receptor 2, AVPR2
XRN1	5'-3' Exoribonuclease 1
Å	Angstrom, 0.1 nanometer

List of papers

Paper I (1)
Holen T, **Moe SE**, Sørbø JG, Meza TJ, Ottersen OP and Klungland A
Tolerated wobble mutations in siRNAs decrease specificity, but can enhance activity in vivo.
Nucleic Acids Research 2005. Vol. 33. No. 15. 4704-4710

Paper II (2)
Sørbø JG, **Moe SE** and Holen T
Early upregulation in nasal epithelium and strong expression in olfactory bulb glomeruli suggest a role for Aquaprorin-4 in olfaction.
FEBS Letters 2007. Vol. 581. No. 25. 4884-4890

Paper III (3)
Sørbø JG, **Moe SE**, Ottersen OP and Holen T
The molecular compositions of square arrays.
Biochemistry 2008. Vol. 47. No. 8. 2631-2637

Paper IV (4)
Moe SE*, Sorbo JG*, Sogaard R, Zeuthen T, Ottersen OP and Holen T
New isoforms of rat Aquaporin-4.
Genomics 2008. Vol. 91. No. 4. 367-377
*These authors contributed equally to this study

Paper V (5)
Moe SE, Sørbø JG and Holen T
Huntington triplet-repeat locus is stable under long-term Fen1 knockdown in human cells.
Journal of Neuroscience Methods 2008. Vol. 171. No. 2. 233-238

Paper VI (6)
Strand L*, **Moe SE*,** Solbu TT, Vaadal M and Holen T
Roles of aquaporin-4 isoforms and amino acids in square array assembly.
Biochemistry 2009. Vol. 48. No. 25. 5785-5793
*These authors contributed equally to this study

Introduction

General Introduction

"...the central dogma is as important today as when it was first proposed"
Francis Crick Nature 1970 (7)

There are currently more than 2,000 published articles on the water channel Aquaporin-4, and even more impressing more than 20,000 publications in the field of RNA interference. Thus, a humble and respectful approach should be applied when pursuing such vast topics in a thesis.

The cell is the fundamental structure of all living organisms, an idea emerging in the nineteenth century (8). Bacteria and yeast are single celled organisms. The male roundworm *Caenorhabditis elegans* has 959 cells. The average human body consists of 10^{13} cells (9), but it starts out with two single cells. To grasp the complexity of life, a fundamental understanding of the cell must be in place. The quest for mechanisms controlling basic cell functions has promoted some of our greatest scientific discoveries.

Nobel laureate Francis Crick proposed in 1958 a theoretical framework for the comprehension of the cell, namely the Central Dogma of Molecular Biology (10). Within the DNA lies the recipe of life, as DNA can be replicated to yield new cells, or it can be translated from a nucleic acid to a protein (Figure 1). Proteins are the main building blocks of the cell. In 2001 the human genome was published (11, 12). It showed that our DNA consists of approximately 3 billion basepairs and roughly 20,000 protein-encoding genes.

To study the function of a single protein, a common strategy is to disrupt its gene expression and study the phenotypic effect. The discovery that cells harbor an innate mechanism for disruption of gene expression was astonishing. The biological process in which small RNA molecules inhibit gene expression is named RNA interference. RNA interference has become an invaluable tool in research and holds great potential for future medicine. Craig Mello and Andrew Fire received the Nobel Prize in Medicine in 2006 for their discovery of RNA interference.

Almost all cells are polarized, for instance they have an apical and a basolateral surface, with different transport capacities (Figure 1). The cell is enclosed by a plasma membrane consisting of a phospholipid bilayer and membrane proteins, which serve as a compartmentalization from the external milieu. As the human body consists of 55- 68% water (13), water movement across cell membranes is of special interest. Rapid water transport occurs through specialized transmembrane proteins. Peter Agre was awarded the Nobel Prize in Chemistry in 2003 for his discovery of water channels. The main brain water channel is Aquaporin-4.

"Science seldom proceeds in the straightforward logical manner imagined by outsiders", stated Nobel laureate James Watson in his book from 1968, *The Double Helix*. Our project originally started as a student project ambitiously entitled "Characterization of a series of siRNA against the water transport channel Aquaporin-

4 and finding a delivery system of siRNA to the rat retina, with the goal of developing new tools for treatment of Brain Edema".

We developed efficient siRNAs against AQP4 in cell lines and also investigated basic mechanisms of mismatches in siRNA (1). The logical continuation of the project was to utilize the best candidate siRNA for direct injection into the rat eye. The rat retina, being an embryonic derivate of the brain, was chosen as the preliminary target for its accessibility and abundant expression of AQP4 and served in theory as an excellent model. Albeit, moving from *in vitro* to *in vivo* proved to be a huge challenge.

Reliable tools for quantifying AQP4 protein were developed (2, 3). While awaiting the breakthrough of our *in vivo* experiments, new project ideas came forth. We remapped the AQP4 rat gene, finding new isoforms (4). Structural hypotheses of AQP4 square arrays could be investigated (6), and better methods to initiate gene silencing could be explored (5).

Our *in vivo* project in the end was not successful. However, eye-injection of naked siRNA for treatment of glaucoma is currently in clinical trials (14), showing that our initial idea was relevant.

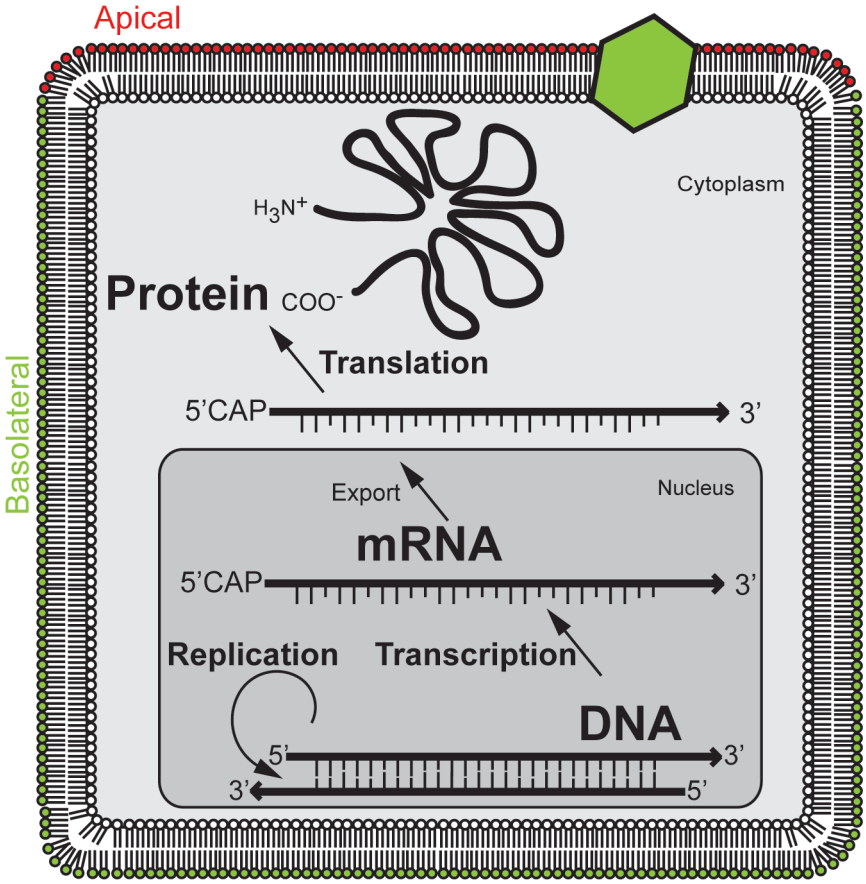

Figure 1: *The Central Dogma*. DNA ➔RNA➔ Protein. Francis Crick launched a framework for the protein synthesis (10); The specificity of a piece of nucleic acid is expressed solely by the sequence of its bases, and that this sequence is a simple code for the amino acid sequence of a particular protein. The figure also shows cell polarity that is it has an apical (red) and a basolateral surface (green). In the upper right corner a transmembrane protein (green) is illustrated.

Introduction to RNA interference

The discovery of RNA interference is one of the milestones of modern biology. The RNAi machinery is conserved through all major eukaryotic lineages. In addition, distinct miRNA pathways have evolved in higher organisms. As some unicellular eukaryotes have lost their RNAi-machinery independently (*Saccharomyces cerevisiae*, *Leishmania major*, *Cyanidioschyzon merolae* and *Plasmodium Falciparum*), RNAi might be dispensable in unicellular eukaryotes (15). However, in multicellular eukaryotes RNAi is essential. This could be due to microRNA (miRNA) contribution in gene regulation (16), and is supported by the fact that loss of one of the key components, either Dicer or Ago-2, promotes embryonically lethality (17, 18).

Plant biologists observed the RNAi phenomenon indirectly in the early nineties (19). In an attempt to get more plant coloration by inserting extra copies of the gene encoding *chalcone synthase* in the petunia-flower, they obtained a contradictory result (Figure 2). Instead of more plant coloration, the plant lost its color. Although the transcription rates were stable, the mRNA stability of the gene was markedly reduced. The authors named these observations "co-suppression" as both the endogenous gene and the transgene were silenced as a consequence of expressing the latter.

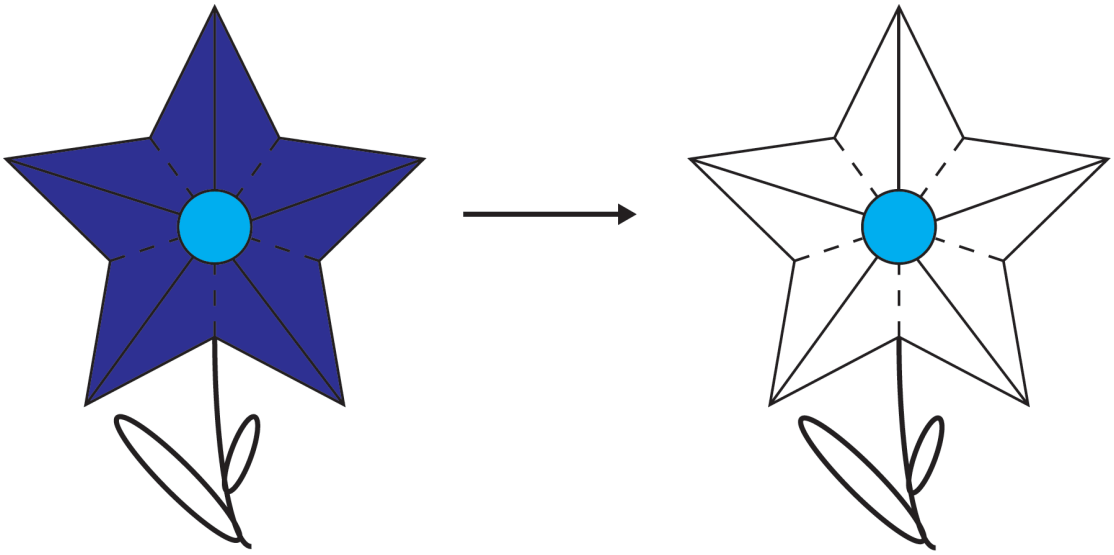

Figure 2: *Post Transcriptional Gene Silencing.* By introducing a vector containing cDNA for the gene responsible for plant coloration in the flower petunia, the plant surprisingly lost its color.

Later, co-suppression was renamed *P*ost *T*ranscriptional *G*ene *S*ilencing (PTGS) as all observations of the phenomenon shared a common feature: the target RNA was depleted after transcription. PTGS is thought to be an innate antiviral defense mechanism and a defense against transposons in plants. It was shown that RNA molecules were the determinants of PTGS, as 25-nucleotide antisense RNA went along with the PTGS phenomenon in various plant lines (20). Today, we name the observed small RNAs small interfering RNAs (siRNA).

The definitive discovery of RNA interference was provided in 1998 (21). Microinjection of *long* double stranded RNA (dsRNA) with homology to the *unc-22* gene in *Caenorhabditis elegans* (*C. elegans*) produced a specific twitching phenotype

in the nematode, mimicking known loss-of-function mutations of this gene. The injection of dsRNA promoted a pronounced decrease in endogenous gene expression. The gene silencing in *C. elegans* spread through cellular boundaries. Indeed, *C. elegans* has turned out to be a particularly good model for studying gene silencing because gene silencing also can be initiated by simply soaking the nematodes in a dsRNA-containing solution or even just feeding them with dsRNA-producing *Escherichia coli* (*E. coli*) (22).

Using extracts from the fruit fly *Drosophila melanogaster*, it was shown that dsRNA ablates target mRNA through a sequence specific nuclease activity and named the enzyme involved *R*NA-*I*nduced *S*ilencing *C*omplex (RISC) (23). The same study showed that in *Drosophila* shorter dsRNA were less effective than longer dsRNA in degrading target mRNA. Further studies using *Drosophila* extracts showed that long dsRNA is processed into smaller 21-23 nucleotide (nt) dsRNAs (24), and this was accomplished by the Dicer nuclease (25).

Surprisingly, it did not seem that scientists could utilize the discovery in lower organisms in mammalian cell systems. Introduction of long dsRNA to mammalian cell systems did not lead to RNAi, but to induction of the interferon response and the protein kinase PKR-pathway. This potent cellular response probably evolved as a potent antiviral defense and may inhibit protein translation and induce apoptosis (26). The inability to induce RNAi by long dsRNA in human cell lines were solved by introducing synthetic 21 nt siRNA with symmetric 2 nt 3' overhangs (27). This discovery allowed application of RNAi as functional tool in scientific research, and was an eye-opener for future use of RNAi in human gene-specific therapy (28, 29). Currently, several RNAi-based drugs are in phase III-trials (14).

Mechanisms of gene silencing

There are three fundamental steps in the RNAi machinery (Figure 3). First the appropriate trigger must be present. Then follows the initiation phase with strand selection and assembly of RISC. The final effector phase involves cleavage of target mRNA. The resulting cleaved fragments of the mRNA have unprotected ends and are subsequently degraded by cellular nucleases.

Natural triggers of RNAi could be repeat-associated transcripts, viral RNAs, gene duplexes and transgene transcripts (30). Genome projects have contributed in identifying other classes of small endogenous RNAs, such as microRNA and PIWI-interacting RNA (piRNA), which employ the RNAi-machinery. A thorough description of these pathways would be beyond the scope of this thesis. Shortly, microRNA constitute an abundant class of small non-protein encoding RNAs encoded for by distinct genes. miRNA has been shown to play important roles in functions as fundamental as development, proliferation, hematopoiesis and apoptosis. Claims have been made that tissue-specific miRNAs help define and maintain the different cell types in mammalians (31).

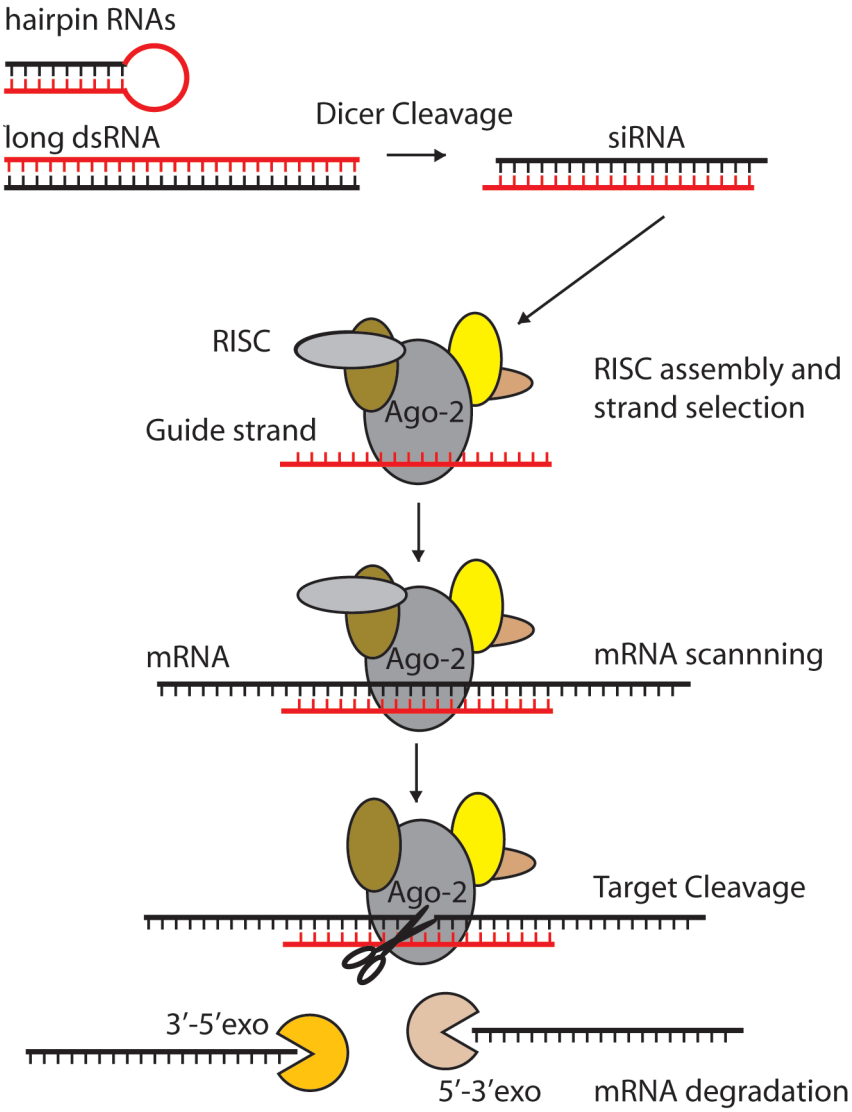

Figure 3: *The RNAi pathway*. The core element in RNAi is known as the RISC. Its key protein is Ago-2. There are different triggers for RISC loading, here exemplified with an shRNA, long dsRNA and an siRNA. Target recognition and cleavage is followed by target release and subsequent degradation of the mRNA through exonucleases.

It is commonly believed that miRNA influences translation in eukaryotes by posttranscriptional downregulation or inhibition of gene expression, although the mechanism is far from simple (16, 32). Whereas siRNAs are fully complementary to their targets, miRNA show limited complementarity to their targets. Thus, it is difficult to predict targets for the different miRNAs, because one miRNA is able to regulate mildly several hundreds of mRNAs (33). PIWI-interacting RNAs are expressed in germ lines and may play a protective role in the germ line genome (34).

The three examples of triggers used in Figure 3 include dsRNA, hairpin RNAs and siRNA. Dicer facilitates cleavage of dsRNA and hairpin RNA to yield siRNA (25). Dicer-mediated cleavage is highly effective, as no intermediates have been observed *in vitro* or *in vivo*. Short interfering RNAs (siRNA) are duplexes of 21-23 nucleotides that are base-paired with 2 nt 3' overhangs and phosphate group at their 5' ends (Figure 4).

Figure 4. *siRNA-duplex.* An example of a 21-nt siRNA duplex with its sense and antisense strands indicated. The antisense strand is complementary to target RNA. There is a 2 nt overhang at the 3' end and a phosphate group at the 5' end.

An siRNA-duplex consists of two strands; the sense strand and the antisense strand. These are in the literature also referred to as the passenger strand and the guide strand, respectively, because the antisense strand is the mediator of target cleavage. Dicer processes natural siRNA from longer dsRNA species through cleavage. More often they are designed and processed by chemical synthesis to be fully complementary to their target (27).

The effect of synthetic siRNA in mammalian cells is transient: the silencing effect is of limited duration. In 2002 several groups showed that siRNA could be expressed intracellularly from DNA plasmids. Taking advantage of the concept of endogenous miRNA as a model, where precursor short hairpin RNA are processed by Dicer into their mature forms used by the RNAi machinery, short hairpin RNAs (shRNA) containing 29 nucleotides of dsRNA and a simple loop structure were effective triggers of RNAi when expressed in cells (35). The vector is expressed by RNA polymerase III to yield an shRNA, which is subsequently cleaved by Dicer yielding a pool of siRNA. This provided an obvious advantage, as one could get a contiguous expression of siRNA by way of stable transfected cells.

The use of vectors also provides the opportunity for regulation through different promoters. Indeed, utilizing the best candidate from our initial screen and the concept of shRNA-based vectors, we created a cell line capable of turning the DNA-repair gene Fen1 on and off simply by adding tetracycline to the growth medium (5). Thus, RNAi is a useful tool in reverse genetics.

Regardless of original trigger, both strands of a siRNA-duplex can direct RNAi. The antisense strand can cleave the complementary sense target, whereas the sense strand can cleave anti-sense target. The assembly of an active RISC involves selection of one of the two strands of the siRNA-duplex. The criteria for strand selection are not currently understood. However, some data have shed light on the strand selection. Analysis of siRNA-duplex sequences show that the thermodynamic stability of their two RNA ends can influence which strand is incorporated into RISC. A duplex less stable in the 5' region than the 3' region of the guide strand, would favor incorporation of this strand into RISC (36). Indeed, low base-pairing stability at the 5' end of the antisense strand characterizes functional siRNA in cultured cells (37). Supportive of this is the demonstration that the RISC enzyme can tolerate more mutations in the 3' end of the antisense than in the 5' end (38). Thus, one of the strategies for designing an effective siRNA is to introduce sequence asymmetry into the siRNA duplex. Strand selection is one of the main hypotheses that predict the effectiveness of an siRNA.

In mammalian cells, a siRNA-duplex is loaded directly into the RISC (39). RISC will then cleave the sense strand. One molecule of sense strand is cleaved for every strand

assembled into RISC. The following dissociation step includes releasing the cleaved sense strand from RISC and thereby facilitating formation of an active RISC complex.

Key components of the human RISC include Argonaute proteins, Dicer, TRPB and the dsRNA-binding protein PACT (30). Nonetheless, the Argonaute is the primary effector of the RNAi machinery. The human Argonaute family consists of 8 members with a central role in RNA silencing. Ago proteins contain two major domains, PAZ and PIWI. All biochemically purified and characterized RNA silencing effector complexes includes at least one Argonaute protein. Ago-2-deficient mice are not compatible with life (18). Ago-2 is the catalytic engine of human RISC, whereas other Ago-family members can associate with siRNA and miRNA but do not mediate cleavage (40). The PIWI domain is responsible for the cleavage of target mRNA. The PAZ domain recognizes the characteristic 3' overhang in siRNA, thereby promoting the loading of siRNA into the RISC (41) (Figure 5).

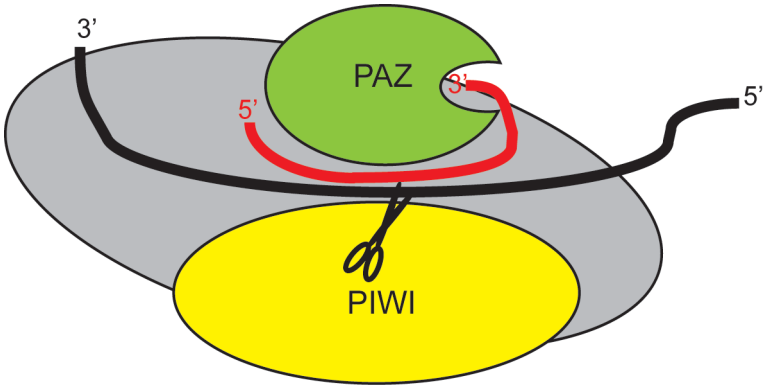

Figure 5: *Ago-2.* Ago-2 is the catalytic engine of human RISC. It is able to cleave mRNA (black) with the aid of the antisense strand (red) *in vitro* without any additional proteins. Ago-2 consists of several subdomains, including the PIWI domain, which resembles RNase H, known to cleave mRNA, and the PAZ domain that binds nucleic acids.

A perfect match between the antisense and an mRNA will initiate cleavage by Ago-2, with a subsequent degradation by nucleases of the cleaved mRNA. Both human and *Drosophila* cleave their target RNAs at the phosphodiester bond located across nucleotide 10 and 11 from the 5' end of the antisense strand (42). After mRNA cleavage, the two fragments of mRNA must be degraded. In a model using *Drosophila* S2-cells it has been shown that mRNA cleaved by RISC had their 5' cleavage products rapidly degraded from their 3' end by the exosome and that the 3' cleavage fragments are degraded from their 5' ends by XRN1 (43). Thus, mRNAs processed by RISC are degraded by exonucleases, starting at both ends of the cleavage site, without undergoing decapping or deadenylation like the classical model of mRNA-degradation (44).

RNA-based medicine: in vivo use of siRNA

Because the coding sequence (CDS) of an mRNA is the most reliable mRNA sequence information available, RNAi-vectors commonly target this region (45). RNAi has been shown in cell lines to deplete almost any mRNA of interest, but the

delivery *in vivo* still remains a major barrier before it can be fully used in clinical settings.

The efficacy of siRNA to silence target mRNA depends on its sequence. This phenomenon is named positional effects. The shifting of only a few nucleotides in the sequence can deteriorate the silencing capacity of a good siRNA (1, 28, 46).

Large screens have provided data for development of algorithms for predicting the efficacy of siRNA. Many are based on the asymmetric selection of strand hypothesis (36, 37), but this hypothesis is probably incomplete, because other domains within the siRNA sequence might play a role. For instance, base-paring energy around the point of cleavage participate (1). Another idea is that secondary structures within target mRNA might influence the efficacy (47).

Some siRNAs tolerate mutations and chemical modification (28, 29). We have investigated the positional effects and the role of wobble mutations in different positions (1). Some siRNAs can tolerate several mismatches, but this increases the risk of unwanted off-target effects (48). Off-target effects are caused by sequence homology to other mRNA transcripts than the target gene. It is currently unclear whether off-target activity is caused by translational repression or mRNA cleavage. There also exist divergent conclusions regarding the specificity of siRNA and the incidence of off-target effects (49-51).

The widespread use of siRNA in functional genomics in cell lines has provided hopes for RNA-based medicine. *In vivo* applications have been more difficult than *in vitro*. *In vivo* use of RNAi could be categorized in two approaches: localized siRNA delivery and systemic administration of RNAi-construct.
The first approach would yield higher bioavailability with less adverse effects and would be an ideal choice in easy accessible targets like the eye, skin and mucosal membranes. In a mouse model it has been shown that intranasal administration of siRNA targeting parainfluenza virus and respiratory syncytial virus replication, indeed protects against lung pathology even after infection (52). Thus, low dose aerosol inhalers containing siRNA could be a future intervention for the common cold.
Systemic administrations still face many obstacles. The most important is that vectors would have to avoid uptake and clearance prior to being delivered to their target site. Examples of impediments are phagocytosis, kidney filtration, enzymatic degradation and toxicity (53). In addition, siRNA can exhibit nonspecific effects *in vivo* by activation of the immune system (54). However, it has been shown that siRNAs are capable of knocking down various disease targets *in vivo*.

In the following section, three examples of these experiments will be explained in brief. The first example will show how topical administration of siRNA can prevent disease in mice. The second example will illustrate how systemic administration of siRNA in mice can prevent disease. The last example will show how systemic administration of siRNA in primates can prevent disease, illustrating the potential role of RNAi-based drugs as a treatment for human disease. Finally, the section will end by briefly mentioning ongoing clinical trials in this domain.

Herpes Simplex Virus-2 (HSV-2) infection causes significant morbidity and can make vaginal epithelium more accessible to HIV-infections. In mouse models intravaginal installation of liposomal siRNA can cause gene silencing throughout vagina and cervix, without causing systemic effects. In a cell system, siRNA against HSV-2 provided a 25-fold decrease in viral replication (55). In their mouse model for HSV-2 infection 75% of the control group died, whereas only 25% died after vaginal installation of siRNA against HSV-2. The protection against this lethal infection lasted up to 9 days both when administrated before and after the HSV-2 challenge. Thus, topical administration of siRNA may protect against lethal viral infections.

Serum levels of apolipoprotein B (ApoB), low-density lipoproteins (LDL) and cholesterol correlate with an increased risk of coronary artery disease. Cholesterol-conjugated siRNA against ApoB demonstrated specific silencing in liver and jejenum of rodents (56). Analyzing the lipoprotein profiles in these mice revealed an above 40% reduction in chylomicrons and LDL-levels, as well as a significant reduction in total cholesterol.

Intravenous delivery of siRNA against the lipid-associate ApoB in liposomes yielded approximately 80% silencing of liver ApoB in primates (57). The mRNA silencing occurred in a dose-dependent manner, with an effect on mRNA-levels lasting up to 13 days. To evaluate if this was an RNAi-phenomenon, the predicted cleavage site was found in the cleaved mRNA using 5' RACE.

Besides the reduction in serum ApoB, the biological effects also included a reduction in blood levels of total cholesterol and LDL. The latter two also occurred in a dose-dependent manner. Better still, no negative side-effects were observed. As the effect was already present after 24 hours, these drugs have a clinical potential. Similar effects were found in a study by Alnylam with systemic administration of an RNAi-construct against PCSK9, an enzyme regulating levels of the LDL-receptor (58). This drug is currently in phase II trials (59).

There are currently about 30 ongoing clinical trials to assess siRNA therapeutics (14). The first RNAi-based drugs will probably be on the market within a few years, as some of these trials are already in phase III development.

In summary, the mechanism of RNAi is that short, double-stranded RNA, named siRNA, are loaded into the RISC-complex. The antisense strand is paired to its complementary mRNA sequence, whereas the sense strand is discarded. Upon siRNA:mRNA-binding, RNAi is induced through cleavage and subsequent degradation or translational repression. There are some limitations to *in vivo* use, and yet there are several unresolved issues, but currently several therapeutics are in clinical trials. We have studied the RNAi machinery in parallel with the goal of utilizing RNA silencing against the brain water channel Aquaporin-4.

Introduction to Aquaporins

Water movement through lipid bilayers and the discovery of Aquaporin-1

Water movement across membranes is accomplished by two mechanisms: simple diffusion through the phospholipid bilayer, and rapid transport through specialized transmembrane transporters. Physiological studies on human red blood cells provided functional evidence for the existence of water channels decades before their discovery, as red blood cells have higher water permeability than any other known cell and any artificial lipid bilayer. In 1957, it was proposed on the basis of water permeability assays and calculations, that red blood cells had water pores of approximately 3.5 Å (60). It was later shown that mercurial agents could reversibly inhibit water transport through red blood cells, suggestive of mercury being a water pore inhibitor (61).

Peter Agre and colleagues discovered the first water channel during biochemical purification of the human erythrocyte Rh blood group antigens. The first characterized molecular water channel was originally named CHIP28, an abundant membrane protein. It had previously stayed undetected due to its poor binding of the conventional coommassie stain, but it became visible using silver stain (62). The cDNA was later found and its amino sequence was deduced (63).

The protein was proposed to consist of 6 transmembrane helices, where the first three bilayer-spanning domains had a reverse orientation of the next three domains, suggestive of a bidirectional active channel. CHIP28 was hypothesized to be the water channel scientists had been looking for in erythrocytes.

The water transport function of CHIP28 was demonstrated upon expression of its complementary RNA (cRNA) in oocytes from the frog *Xenopus laevis*, where it lead to increased osmotic water permeability, causing the cell to swell and burst in hypotonic medium. The swelling was reversibly inhibited by mercuric chloride (64). The hourglass model was indicated for CHIP28 (65). It was suggested that the functional name "aquaporin" should be used for the discovered and yet-to-be discovered water channels (66). Peter Agre received the Nobel Prize in Chemistry in 2003 for the discovery of aquaporins.

The water channel family

Aquaporins are a family of sequence-related transmembrane proteins. 13 mammalian aquaporins have been discovered (AQP1-12 plus "AQP0"). There are homologous water channels in bacteria, plants and other organisms (67). The aquaporins are believed to be essential for water- and osmoregulation in plants, microbes and mammals. All the aquaporins seem to reflect the different need for cells and organs to control their individual needs for water balance. The size of each monomer is approximately 30 kDa. All aquaporins have N- and C-terminals facing the cytosol and they all contain 6 transmembrane helical domains connected by five loops (65, 68) (See Figure 6: AQP4). These membrane-spanning helical domains surround the water pore. The water pore permits bidirectional water transport (69).

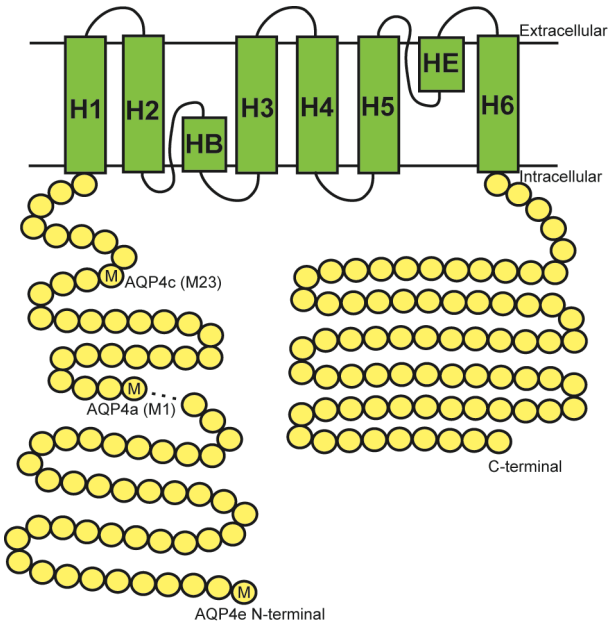

Figure 6: *Structure of rat AQP4*. AQP4 is a transmembrane protein with six transmembrane helices (H1-6). The novel isoform AQP4e has a longer N-terminal, actually 41 amino acids longer than AQP4a (M1). The distinction between Aqp4a and AQP4c (M23) is the 22 N-terminal amino acids.

Aquaporins generally form tetramers (70). The lens fiber protein *M*ajor *I*ntrinsic *P*rotein, MIP, also sometimes called AQP0, and AQP4, the latter being the main brain water channel, can also form large aggregates known as square arrays. A thorough review of all the different aquaporins is beyond the scope of this thesis. However, a brief summary will follow. See Table 1 for an overview of mammalian aquaporin distribution in different tissues and organs.

Aquaporins can be subdivided into aquaporins and aquaglyceroporins based on their substance permeability (68). The first group functions primarily as water-selective transporters and includes AQP1, AQP2, AQP4, AQP5 and AQP8. Aquaglyceroporins, which in addition to water also transports glycerol, includes AQP3, AQP6, AQP7, AQP9 and AQP10 (67). A third category named superaquaporins or unorthodox aquaporins has also been suggested based on their primary sequence. This group includes AQP11 and AQP12 (71). Aquaporins are essential for fluid transport across epithelium, which is reflected in studies from knockout-mice.

Some examples should briefly be mentioned: AQP5 is expressed apically in epithelial cells of serous acini in salivary glands. Saliva from $AQP5^{-/-}$ mice is hypertonic, more viscous and its production is markedly reduced (72). AQP3 is located in the basal layer of skin keratinocytes and $AQP3^{-/-}$ mice show impaired skin hydration, skin elasticity and slow wound healing (73). AQP7 is expressed in adipocytes, and mice deficient of AQP7 become obese and develop a progressive adipocyte hypertrophy and insulin resistance (74).

Aquaporin	Permeability	Tissue distribution	Subcellular distribution
AQP0 *MIP-26*	Water (low)	Eye lens fiber cells	Plasma membrane
AQP1 *CHIP-28*	Water (high)	Erythrocytes, kidney tubules, lung, vascular endothelium, choroid plexus, ciliary epithelium, intestinal lacteals, corneal endothelium	Plasma membrane
AQP2 *WCH-CD*	Water (high)	Kidney collecting duct, male reproductive tract, endolymphatic sac in the ear	Apical plasma membrane Intracellular vesicles
AQP3* *GLIP*	Water (high), Glycerol (high) Urea (moderate) Ammonia	Kidney collecting duct, epidermis, erytrocytes, airway epithelium, conjunctiva,GI tract, urinary bladder	Basolateral membrane
AQP4 *MIWC*	Water (very high)	Astroglia in brain and spinal cord, skeletal muscle, kidney collecting duct, airways, glandular epithelia, nose, GI tract, retina	Basolateral membrane
AQP5	Water (high)	Salivary gland, lacrimal gland, sweat gland, alveolar epithelium, corneal epithlium, GI tract, nose	Apical plasma membrane
AQP6	Water(low) Glycerol Urea Anions	Kidney collecting duct intercalated cells	Intracellular vesicles
AQP7*	Water (low) Glycerol (high) Urea (high) Ammonia	Adipose tissue, testis, skeletal muscle kidney proximale tubule	Plasma membrane
AQP8	Water (high) Urea (?) Ammonia	Testis, kidney, liver, pancreas, GI tract, heart, salivary gland	Plasma membrane Intracellular vesicles
AQP9*	Water (low), Glycerol (high) Urea (high) Ammonia	Liver, leukocytes, testis, brain?, adipose tissue	Plasma membranes
AQP10*	Water (low) Glycerol (high) Urea (high)	Gastroinstestinal tract, adipose tissue, male reproductive system, skin	Intracellular vesicles
AQP11**	Water (?) Glycerol	Testis, thymus, kidney, liver, brain?	Intracellular
AQP12**	?	Pancreatic acinar cells	Intracellular

Table 1: *Distribution of mammalian aquaporins.* The table is based on reviews in the field (68, 75, 76). AQP0 is also known as *M*ajor *I*ntrinsic *P*rotein; AQP1 was formerly known as CHIP28; AQP2 as *W*ater *Ch*annel of *C*ollecting *D*uct; AQP3 as *Gl*ycerol *I*ntrinsic *P*rotein and AQP4 as MIWC. * Aquaclyceroprotein. **Superaquaporin.

Aquaporins in the kidney

The kidney proximal tubules and renal collecting duct principal cells are well defined for their aquaporin-physiology and serve as good examples for the general understanding of water channels. The kidneys are essential for regulation of water homeostasis as well as blood pH and elimination of toxic substances. The kidneys receive about 20% of cardiac output and the human glomerular filtration rate is about 150 L/day, where >99% is reabsorbed. The functional unit of the kidney is the nephron (77). Each kidney includes about one million nephrons and each segment of the kidney has distinct water transport capacity and distinct aquaporins.

Blood filtrate will be lost to the urine if not reabsorbed fast enough. Aquaporins facilitate fast water transport. This is reflected in mice lacking AQP1, AQP2, AQP3 or AQP4 all have some degree of defective urinary concentrating ability (78-81). Deletion of AQP2, AQP3 and to some degree AQP4 reduces collecting duct water permeability. The lack of water channels in different kidney segments results in ineffective reabsorption and fluid escape into the urine.

In proximal tubuli more than 75% of the glomerular filtrate water is reabsorbed into vasculature via the AQP1 pathway. In the proximal tubule and the thin descending limb, AQP1 is abundant in both apical and basolateral membranes, as well as in the endothelium of vasa recta (82, 83). Hence AQP1$^{-/-}$ mice have severe polyuria and poor ability to concentrate urine (78).

Some rare human mutations of AQP1 do exist. Surprisingly, these subjects have no obvious clinical features such as polyuria, which is suggestive of a species difference between rodents and humans (84). Normal individuals respond to overnight thirsting by concentrating their urine to a maximum of 1200 mOsm kg^{-1}. AQP1 null individuals cannot concentrate urine to more than 460 mOsm kg^{-1} even after 24 hours of thirsting (85). This indicates that AQP1 plays an important role in renal concentration also in humans.

There are no water channels in the ascending loop of Henle. The absence of water channels in this region accounts for the low osmotic permeability in this segment.

The final volume and concentration of urine is determined in the renal collecting ducts, in which there is a well-defined transcellular pathway for water. Water from the tubular lumen can cross through AQP2 channels apically, and thereafter exit through constitutively expressed water channels basolaterally, before final reentry into the circulation (Figure 7). Throughout most of the collecting ducts, the basolateral water channel is AQP3. Some AQP4 is located in collecting ducts of the inner medulla.

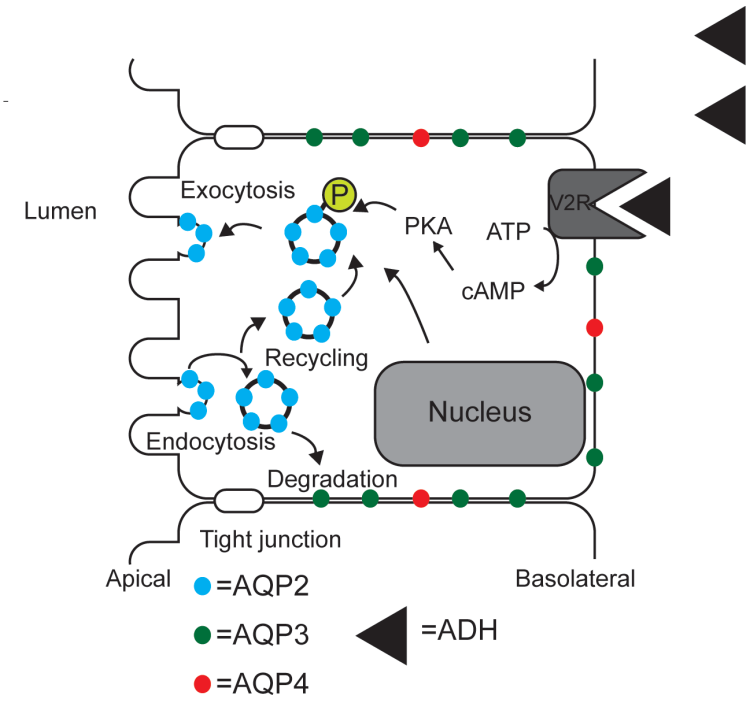

Figure 7: *Aquaporins in kidney collecting ducts*. The posterior pituitary gland releases ADH into the bloodstream as a response to dehydration, ADH acts on a V2A-receptor in the collecting ducts. The receptor activates intracellular signaling cascades. The result is translocation of AQP2 from intracellular vesicles towards the apical plasma membrane, thus providing a transcellular pathway for H_2O from the inner lumen and back into the bloodstream through the basolateral water channels AQP3 and AQP4 (inner medulla). Adapted from a review in the field (86).

Hormonal regulation of cellular location of AQP2 determines urine concentration

The final urine concentration is determined by the presence or absence of anti-diuretic hormone (ADH, also known as arginine vasopressin). ADH is released from the pituitary gland when the body is dehydrated, and ADH increases water permeability of the collecting ducts (87). The hormone binds to the V2-receptor, located in the principal cells of the collecting ducts, and which is coupled to a G-protein. Adenylyl cyclase converts ATP to cAMP and activates the protein kinase A (PKA)-pathway. PKA phosphorylates AQP2 at the carboxy terminus (86, 88).

By phosphorylation activation, intracellular vesicles with AQP2 are docked to the plasma membrane, thereby contributing to a water pathway from the lumen through the principal cell and back into the blood stream. AQP2 null mice have impaired neonatal survival (80). Nephrogenic diabetes insipidus (NDI) is a condition in which the affected are unable to concentrate urine in response to ADH. Mutations have been identified at both the first and last stages of the pathway for ADH-induced antidiuresis. In X-linked NDI there are mutations in the gene encoding the V2-receptor (89). AQP2 mutations are associated with non-X-linked congenital NDI (90).

$AQP3^{-/-}$ mice have severe polyuria (81). These mice have a 10-fold increase in fluid consumption when given free access to water, probably as a consequence of their inability to concentrate urine properly. Deletion of AQP4 produces only a mild defect in the ability to concentrate urine (79). The mild phenotype is probably due to the relatively low expression of AQP4 in the kidneys. The kangaroo rat *Dipodomys*

merriami can concentrate their urine up to 6000 mOsm/L, although this rodent lacks AQP4 in the kidney (91). This observation further supports an argument against a strong functional role of AQP4 in the kidneys.

Aquaporins in the brain

As the kidneys play a major role in body fluid homeostasis, the need for rapid water transport is relatively easy to understand. The human brain, however, has no known need for rapid water transport. The only major fluid flux is the production of cerebrospinal fluid (CSF), which occurs at a rate approximately 0.5 L/day. Yet, the concentration of water channels in the human brain appears higher than in the kidney.

AQP4 is concentrated in the astrocyte end-feet surrounding blood vessels (Figure 8). Potential water transport capacity of AQP4 is surprisingly high in the brain. AQP1 is mainly located in the choroid plexus (92), whereas AQP4 is mainly located around blood vessels (93, 94). AQP1$^{-/-}$ mice show no morphological alteration of their choroid plexus, but they have reduced intracranial pressure (95). Their CSF production is also reduced 25% *in vivo*, arguing for at least a partial role of AQP1 in CSF production.

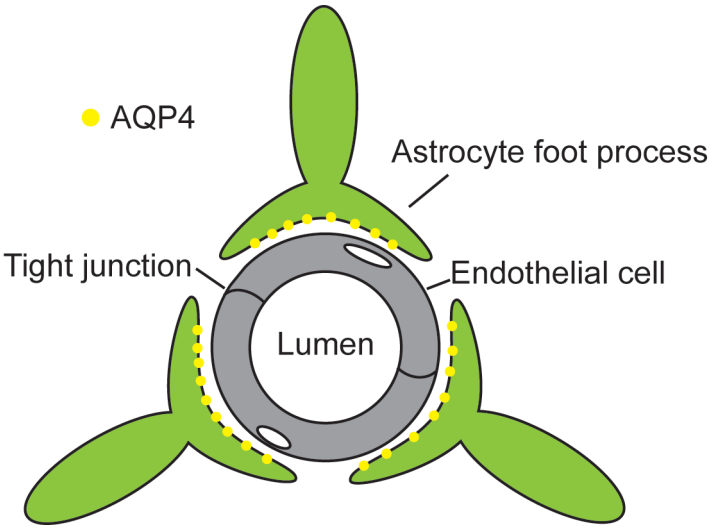

Figure 8: *The blood-brain barrier*. The endothelial cells are connected with tight junctions. No AQP have been located in the endothelial cells that make up the BBB. AQP4 is located in the astrocytic end-feet that surround the blood vessels.

Some reports have suggested the presence of AQP9 in neurons in the mesencephalon (96), although this is controversial (97). Thus, any potential role of AQP9 in the brain will not be further discussed.

A feature of AQP1 throughout the body is its localization in the endothelium of blood vessels, the major exception being the brain blood vessels. No other aquaporins have been located in the endothelium of the blood-brain barrier. Extensive tight junctions connect the endothelial cells, weakening the hypothesis that water moves paracellularly. Hence, as there is no known transcellular pathway for water transport, rapid water movement across the blood-brain barrier is difficult to understand.

The brain water channel AQP4

All the different AQPs have different water permeability, but AQP4 differs from the others having been reported to have at least four times higher intrinsic water permeability then the other homologues (98). The first AQP4 isoform was cloned from a rat cDNA library in 1994 and it was shown to increase water transport in a mercurial-insensitive manner in *Xenopus* oocytes: originally named *M*ercury *I*nsensitive *W*ater *C*hannel, MIWC (94). AQP4 was also cloned from a rat brain library, and here two isoform named M1 and M23 were identified (99).

We have later shown that there are 6 isoforms of AQP4 in the rat brain (4) and shown that some of the isoforms interact at a molecular level (6). Cloning of cDNA from human material has so far only indicated two isoforms (100).

AQP4 is also expressed several other places in the body, such as at the basolateral membrane of kidney collecting ducts, gastric parietal cells, salivary and lacrimal glands, colon, lung, trachea and skeletal muscle sarcolemma (101-103). However, AQP4 expression in tissues outside the brain is generally at a low level, and with an uncertain physiological function. As mentioned, deletion of AQP4 causes only a mild defect in urinary concentration ability (79). For another example, AQP4 null mice had no difference in osmotic water permeability of muscle cells, no difference in muscle force generation, treadmill performance or muscle swelling compared to the wild type mice (104).

Early reports indicated that AQP4 is expressed in cells present at or near fluid interfaces: in astrocytes near the blood-brain barrier and glia limitans, and in the ependymal cells lining the brain ventricles (93, 101, 102). The expression is high in gray matter of the spinal cord, in Müller cells in the retina and in supporting cells of the inner ear. We have studied the location of AQP4 in the olfactory system. Here AQP4 is strongly expressed in the olfactory gland of Bowman and in the glomeruli of the olfactory bulb (2, 105).

AQP4 was first cloned in 1994, however, the protein is organized in supramolecular complexes known as square arrays and had been studied in the brain for decades by freeze-fracture electron microscopy (106). The striking feature of square arrays, and thus AQP4, is their superabundant expression in the brain, with up to 40% of the total surface of capillary end-feet covered by square arrays (106).

Square arrays are intramembrane particles formed as regular square lattices, and they are also known as orthogonal array of particles (OAPs). Freeze-fracture identified square arrays in a variety of tissues, but the most abundant expression of square arrays were in brain astrocytes. The description of square arrays originated in the seventies (107). Due to the abundance of square arrays in astrocytes, they were proposed to be utilized for astrocyte identification in specimens (108). Where astrocytic perivascular end-feet contact the basal lamina, the density of OAPs is very high, but when the membrane loses contact with the basal lamina, the density drops to zero (109). It was also shown that square arrays were labile in response to circulatory arrest (110), although these results have been questioned (106).

The connection between AQP4 and square arrays were discovered due to similar tissue distribution (102). This was supported by the fact that rat AQP4 expression in

CHO-cells promoted large assemblies visualized by freeze-fracture. Furthermore, square arrays are absent in AQP4$^{-/-}$ mice (111). By transfecting AQP1-5 in CHO-cells it was demonstrated that only AQP4 was organized in orthogonal arrays (112). Moreover, freeze-fracture immunolabelling directly identified AQP4 as the molecular constituent of square arrays (113).

Rash and colleagues demonstrated the impact of AQP4 isoform on square array structure (114). Whereas an average astrocyte membrane contained 17 intramembrane particles (IMP), in transected cell lines the isoform M1 yielded an average of 2 IMP and M23 produced 78 IMP. Combining M1 and M23 in CHO-cells yielded an average of 6 IMP. This was the first evidence of influence on square array formation by the two most abundant isoforms of AQP4. Later, the idea of isoform-influence on square array formation was investigated further by examining which of the 22 N-terminal amino acids in M1 is vital for square array formation, in an attempt to explain the difference observed between the two isoforms (115).

We have established a method for detection of square arrays by the immunoblotting technique Blue Native PAGE (BN-PAGE), and thereby finding an alternative approach to study them (3, 6). Many questions remain regarding square array size regulation and the function of square arrays.

Hypotheses on the function of AQP4 in the brain

The first AQP4$^{-/-}$ mice showed no difference in development, survival, growth and neuromuscular function (79). The only phenotype observed is a mild defect in urinary concentration and it has also been found to have a mildly expanded extracellular space in the brain cortex (116-118). Deletion of AQP4 does not seem to provide any other structural abnormalities of the brain, nor does it change the integrity of the blood-brain barrier, in two different AQP4-KO mice (119-122). Brains from AQP4-KO exhibited slightly higher basal water content than brains from control mice (120, 122).

In addition to the two above-mentioned AQP4$^{-/-}$ mice, there exists a third AQP4-KO mouse. The Nanjing AQP4-KO mice may exhibit several gross abnormalities in contrast with the other two, including disruption of the blood-brain barrier (123), and increased mortality and neurological deficits in response to transient middle cerebral artery occlusion (124).

There are also studies from other gene-specific knockout animals used to indirectly assess AQP4 biology, such as mice deficient in dystrophin, α-syntrophin or agrin. The results and validity of these studies must be interpreted cautiously, because they are complicated by the fact that dystrophin-KO models shows an increased BBB permeability(125), α-syntrophin$^{-/-}$ shows alteration of other transmembrane proteins such as Kir4.1 (126) and agrin-null mice has a lethal phenotype (127).

Thus, the exact role of AQP4 in the brain remains unclear. The apparently normal phenotype of AQP4 null mice contrasts strikingly with the high abundance, the specialized distribution and the peculiar organization of AQP4 into square arrays. AQP4 has been hypothesized to have the following distinct roles in brain functions:

- Brain water fluxes during pathological conditions
- Cell migration
- Upregulation in brain tumors
- Cell adhesion
- Gas exchange
- Neuro-excitation
- Waste clearance
- A pathological role in neuromyelitis optica

Brain water fluxes during pathological conditions

AQP4 is distributed throughout the brain macroscopically. AQP4 expression is primarily located in the glial cell membrane with the most abundant expression in perivascular glial processes (93). AQP4 is also found in the ependymal and pial cells lining the ventricular system and the subarachnoid space to a smaller extent. However, the hallmark of AQP4 brain distribution is the highly polarized expression in astrocytic foot processes near blood vessels (Figure 8). Localization of AQP4 in the proximity of fluid interfaces, has led to speculations of a role for APQ4 in regulation of cerebral water balance. The proposed role of AQP4 in brain water flux comes for the most part from studies in knockout mice.

Brain edema may be defined as a pathologic increase in total brain fluid content with a following increase in brain tissue volume (128). Cerebral edema leads to increased intracranial pressure, which potentially could lead to ischemia, herniation and death.

Klatzo defined two main types of brain edema: vasogenic and cytotoxic (Figure 9). Vasogenic edema occurs when the blood-brain barrier is disrupted causing a net flow of water along a hydrostatic pressure gradient from the blood into the brain. Vasogenic edema follows tumors, inflammatory lesions and traumatic tissue damage (129).

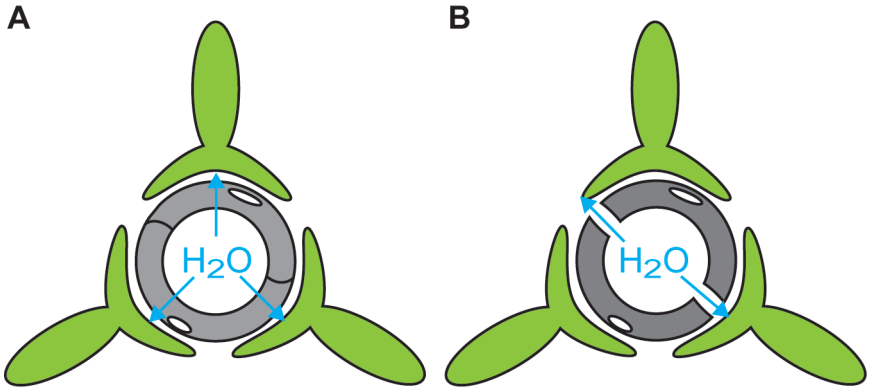

Figure 9: *Brain edema*. A. Cytotoxic brain edema is characterized by cell swelling. Excess water moves through an intact blood-brain barrier by osmotic forces. B. Vasogenic edema is characterized by leaky vessels, that is, the BBB is disrupted and hydrostatic forces drive water from the vasculature and into the extracellular space.

Cytotoxic brain edema is characterized by cellular swelling with the blood-brain barrier still intact. It is often seen in early cerebral ischemia, metabolic derangements or in hyponatremia.

Current treatment of brain edema remains empirical and focuses on optimizing perfusion, minimizing brain metabolic demands and avoiding exacerbation of the osmolar gradient. Basically, there exist two main treatment options (130). The first is conservative management with a transient hyperosmolar agent such as mannitol. The other option is neurosurgical decompression or hemicraniectomy, in which edematous tissue is allowed to expand. Increased knowledge about brain water homeostasis may reveal new therapies for brain edema.

The role of AQP4 in cytotoxic edema

Rapid intraperitoneal injection of water and an ADH-analogue produces severe hyponatremia and subsequently cytotoxic edema. In the acute phase, mice injected with water become paralyzed and will eventually die. Survival after water intoxication was strikingly improved in AQP4-null mice (119). Whereas only 8% of the wild type mice survived this water challenge, 76% of $AQP4^{-/-}$ mice survived. Moreover, the mice showed less symptoms of neurological deficits, less pericapillary swelling of astrocytes, and less brain water accumulation. Supportive of this, transgenic AQP4 overexpression in mice worsens brain swelling in water intoxication (131).

The study by Manley *et al.* also showed that after brain ischemia caused by permanent middle cerebral artery occlusion, there was improved clinical outcome and significantly reduced brain swelling. In accordance, improved survival of AQP4 null mice have been obtained for transient occlusion of left common carotid artery (132), transient bilateral carotid artery occlusion (133) and transient 4-vessel occlusion reducing cerebral blood flow >94% (134).

The protective role of AQP4-deletion was also demonstrated for acute bacterial meningitis (135). By injecting *Streptococcus pneumoniae* into the cerebrospinal fluid, $AQP4^{-/-}$ mice had lower intracranial pressure, brain water accumulation and improved survival. Hence, deletion of AQP4 could improve the clinical outcome of stroke, meningitis and cerebral edema, which is interesting in light of the unknown physiological function of AQP4.

The role of AQP4 in vasogenic edema

Evidence points towards a protective role of AQP4 in vasogenic brain edema. By use of three different models of vasogenic edema; fluid-infusion in brain parenchyma, focal cortical freeze-injury and melanoma cell injection, Papadoupolus *et al*. showed that AQP4-deficient mice have a marked increase in intracranial pressure together with increase in brain water content and accelerated neurological deterioration (120). Brain abscesses are also associated with local vasogenic edema. In a model for brain abscesses, whereby *Staphylococcus aureus* was injected into the striatum causing focal abscesses, there was a significantly worse clinical outcome for AQP4 knockout mice (136).

Greater swelling and worsened neurological outcome were also shown in a model of spinal cord contusion where probably vasogenic edema predominates (137). This holds for a protective role for AQP4 in vasogenic edema. AQP4 may also provide a pathway for ventricular fluid into cerebral microvasculature when primary ventricular pathways are blocked. In a model for progressive obstructive hydrocephalus, by

injecting kaolin to cisterna magna, AQP4-deficient mice had an accelerated ventricular enlargement and elevation of intracranial pressure (138). Also, AQP4 null mice developed more brain swelling and worse neurological score than wild type mice in a model of subarachnoid hemorrhage (139). Enhancers of AQP4 might probably reduce brain swelling in vasogenic edema or hydrocephalus.

Eclampsia

Another related disease where AQP4 has been proposed to be involved is eclampsia. Eclampsia is a hypertensive disorder of pregnancy with the clinical features of tonic-clonic seizures. Because women developing eclampsia often are normotensive prior to the pregnancy, it was proposed that AQP4 was upregulated during pregnancy and in the postpartum period (140). Acute hypertension during pregnancy promotes forced dilatation of brain arterioles and these authors observed a 22-fold upregulation of AQP4 protein compared to non-pregnant controls. In a follow-up RT-PCR study it was proposed that the increased expression of AQP4 was localized in the posterior cerebrum and cerebellum (141). The authors also reported changes in regional expression of AQP1 and AQP9. The increase in AQP4 was thought to enhance water transport across the endothelium during acute hypertension, thereby leading to multifocal vasogenic edema and the neurological complications observed during this condition. However, we were unable to reproduce this finding in pregnant rats using TaqMan real-time RT-PCR and high-quality immunoblotting. Nor did we observe any differences between postpartum rats and male controls (2).

Cell migration

AQP1 was shown to contribute to tumor angiogenesis by increasing endothelial cell migration (142). This observation prompted the hypothesis that aquaporins could be involved in glial scarring, a process where reactive astroglia migrate towards a focal lesion in response to an injury. Comparing wild type and AQP4 deficient mice showed that $AQP4^{-/-}$ astroglia had slower migration *in vitro* and *in vivo* (143, 144). More recently, it has been shown that it is probably the shorter isoform AQP4a (M1) that facilitates astrocyte migration through preferential recruitment at the leading edge, whereas AQP4c (M23), being mostly immobile, is largely confined to nonlammelipodial regions (145).

Upregulation in brain tumors

There is an upregulation and redistribution of AQP4 in malignant human astroglia tumors (146-148). However, no association between AQP4 expression and survival was found in patients with astrocytomas (148).

Cell adhesion

AQP4 has also been suggested to serve as a weak adhesion molecule based on the crystal structure and the observation of increased clustering of AQP4c (M23)-transfected L-cells (149). Consistent with this hypothesis, the predominant lens fiber protein AQP0 can function as an adhesion molecule (150). However, Verkman's group refuted this hypothesis by showing no evidence for increased aggregation by AQP4 expression using multiple assays (151).

Gas exchange
There have been some indications that AQP4 may mediate gas transport. Transfection of oocytes with AQP4 mRNA increased membrane permeability for CO_2, but not NH_3 (152). Molecular dynamics stimulations suggest that NO and O_2 can pass through the four monomers of an AQP4 tetramer, although the water channel is even more conductive for gas through the central pore between the four monomers (153). In agreement with the possibility of AQP4-mediated O_2 transport, it was shown that AQP4 $^{-/-}$ mice have impaired oxygenation in areas remote from brain microvessels (154). However, a gas-conducting role of aquaporins is debated, as there has been found no physiologically significant aquaporin-dependent CO_2 transport in mammalian lung or kidney (155).

Neural signal transduction
Electrophysiological studies in AQP4 null mice have shown that these mice have:

- Mildly impaired vision (156)
- Impaired hearing (157)
- Impaired olfaction (158)
- Slow K+ reuptake after initiation of cortical spreading depression (159)
- High threshold for epileptic seizures and longer epileptic seizure duration and intensity (160)

These observations point towards altered potassium kinetics in the AQP4 deficient mice. The indirect lines of evidence point to a link between AQP4 and inwardly rectifying K^+ channel Kir4.1; the precise co-localization of AQP4 with Kir4.1 (161), the K^+ spatial buffering is accompanied by changes in extracellular space and the observed delay in K^+ clearance in animals and humans with no perivascular AQP4 (162, 163).

However, the proposed functional interaction of AQP4 and the potassium channel Kir4.1 was ruled out by patch-clamp analysis of Müller cells in AQP4 null mice (164) and in astroglia cells from hippocampus (165), where function and expression of Kir4.1 was unaltered in mice lacking AQP4. Another possible hypothesis for the altered potassium kinetics observed in the AQP4 null mice might be that excess K^+ in brain extracellular space (ECS) is taken up by AQP4-positive astrocytes, thereby driving osmotic water influx. This is accompanied with a subsequent shrinkage of ECS to maintain the electrochemical driving force for K^+ reuptake (166).

Waste clearance
The brain has a high metabolic rate and lacks a conventional lymphatic system. Recycling of cerebrospinal fluid could serve as a kind of cerebral lymphatic system. AQP4 has been suggested a major contributor in CSF recycling. Utilizing two-photon laser scanning microscopy and intra-techal administration of fluorescently labeled tracers in mice, the authors proposed a new anatomic fluid pathway facilitating cerebrospinal fluid (CSF)-interstitial fluid (ISF) exchange and clearance of interstitial solutes from the brain (167). The study suggests that a large proportion of subarachnoid CSF recirculates through the brain parenchyma. By suggesting that the perivascular space serves as lymphatics of the brain through the involvement of glial cells, the authors coined the phrase the "glymphatic system". This pathway includes

three elements: (1) a para-arterial subarachnoid CSF influx route to the brain interstitium via the Virchow-Robin spaces: (2) a para-venous ISF clearance route along the large caliber veins: and (3) a trans-parenchymal AQP4-dependent bulk flow pathway in-between.

CSF and interstitial solute clearance were dramatically reduced in $AQP4^{-/-}$ mice. In a subsequent study they show that CSF recirculation is reduced by 95% in the wake state as compared to the sleeping state (168). CSF tracers, such as the neurotoxic metabolite soluble amyloid β, were cleared two-fold faster in mice during sleep. Efficient clearance of metabolites through an AQP4-dependent pathway during sleep is therefore suggested as the physiological role for sleep in all animal species.

A pathological role in neuromyelitis optica

A pathophysiological condition in which AQP4 plays a central role is neuromyelitis optica (NMO), also known as Devic's disease or optic-spinal multiple sclerosis. It is a severe demyelinating disease causing severe disability, including blindness through optic neuritis and paralysis through transverse myelitis. The disease resembles multiple sclerosis (MS), and was long thought to be a variant of multiple sclerosis. However, the patients lack intrathecal IgG-synthesis, but have NMO-IgG in their serum, or more seldom in the cerebrospinal fluid (169). Typically, NMO-patients have worse outcome than MS, as the recoveries of attacks often are incomplete causing permanent damage to the nerve cells (170).

The main target antigen of NMO-IgG is astrocytes close to the blood-brain barrier (171). NMO-sero-positivity is nearly 100% sensitive and specific for NMO (172). Lennon *et al.* was the first to show that NMO-IgG has specific binding to AQP4 (173). This was the first study to implicate AQP4 in the pathogenesis of any autoimmune disorder and the first evidence of an autoantigen marker in a human CNS demyelinating disorder.

Whether AQP4 is just a disease-marker or NMO itself is an autoantibody-mediated disease, is currently debated. The beneficial effect of plasmapheresis supports the notion of a causative role for AQP4 autoantibodies in NMO. The AQP4-specific serum IgG is the subclass IgG_1, a major complement-activating IgG subclass in man. NMO-IgG binds to the extracellular epitope of AQP4 (174). NMO-IgG binding affinity is greater in cells expressing AQP4c (M23), although measurable NMO-binding to AQP4a (M1) can be found (175). Thus, clustering of AQP4 in square arrays might play a role for activation of human complement. It has been shown that the antibodies are found in a ratio 1 (CSF) to 500 (serum) (169). In mice and *in vitro*, NMO-IgG binding to AQP4 causes complement-dependent cytotoxicity when human complement is present (174, 176). Neuro-inflammatory lesions were not found in $AQP4^{-/-}$ mice (176). An argument against the pathological role of AQP4-antibodies is that AQP4 is not expressed in oligodendrocytes (177), although, secondary demyelination might occur in response to the inflammatory response in close proximity. Another argument is that AQP4 is expressed at low levels in different organs like skeletal muscle, kidney, lung and stomach, and these organs show no signs of affliction despite the abundance of NMO-IgG in the blood stream.

Impaired olfactory function has been found as an early manifestation of MS (178). In a pathological study, olfactory bulb and olfactory tract demyelination were found to be a frequent, early and specific manifestation in demyelinating diseases (179). In a recent study 5 of 10 patients with NMO showed olfactory dysfunction, and prevalence was higher in AQP4-antibody-positive patients than in negative ones (180). However, these findings have not been confirmed in a large number of patients. We found that AQP4 is strongly labeled in Bowman glands, basal cells and lamina propria of olfactory epithelium, and also in the glomerular layer of olfactory bulb (2). Upon these findings we proposed a role of AQP4 in olfaction. Subsequently, it was shown that $AQP4^{-/-}$ mice indeed have impaired olfaction (158). Based on our findings and the high AQP4 antibody titer observed in NMO-patients, it is tempting to speculate that the olfactory dysfunction observed in NMO-patients might be a clinical trait of the disease.

In summary, the discovery of aquaporins provided a basis for understanding of fast water movements through cells. Aquaporins play an important role in the kidneys, where rapid water transport is known to occur. The main brain water channel is AQP4. However, its role in the brain is not easy to comprehend and there exist several different hypotheses. We have studied AQP4 at a molecular and anatomical level and contributed to further knowledge in the field, although our initial goal was to utilize RNA interference against Aquaporin-4 *in vivo*. During development of our RNAi method, we also investigated one of the hypotheses regarding the famous neurodegenerative disease, Huntington's disease.

Introduction to Huntington's disease

"...when once it begins it clings to the bitter end"
George Huntington Med Surg Rep 1872 (181)

George Huntington first described chorea of hereditary type as a medical curiosity. He emphasized three marked peculiarities of this disease: its hereditary nature, a tendency to insanity, and as a grave disease only in adulthood (181). He also claimed that no treatment was available and its pathology was unknown. Although today, nearly 150 years later, the gene responsible for Huntington's disease has been found, little is known of the gene's function, and there are no disease-modifying agents.

Huntington's disease (HD) is an autosomal dominant progressive neurodegenerative disease caused by a CAG-repeat expansion in the huntingtin gene (182). Symptoms include progressive motor disability and psychiatric disturbance. Huntingtin is a ubiquitously expressed 348 kDa protein with unknown function. Deletion of both huntingtin alleles is lethal *in utero* (183). The N-terminal of exon 1 in the protein contains a polyglutamine triplet repeat (polyQ). As in all 9 neurodegenerative polyglutamine disorders, including HD, the onset of the disease is strongly dependent on the length of triplet repeat expansion, but the duration of the disease seems independent of repeat length.

How the widely expressed mutant polyQ can cause highly selective neuronal toxicity is a core question. The most affected neuronal type in HD is the neostriatal medium-sized spiny neuron, which can be reproduced in transgenic mice (184). Currently, studies from transgenic mice favor a "two-hit" hypothesis involving cell-autonomous toxicity and abnormal cell-cell interactions (185). The "toxic fragment hypothesis" is based on the unusual appearance of nuclear inclusions within the cells, especially in striatum with mutated huntingtin (186), and the fact that repression of transgene expression of mutant protein can reverse aggregate formation and progressive motor decline (187). In support of this in a proof-of-concept study adenovirus-delivered shRNA that reduced pathologic huntingtin in the striatum and improved behavioral phenotypes in HD mice (188). Thus, RNA interference holds a promise for future therapy for HD. Recently, it has been shown that phosphorylation of serine 13 and 16 in mutant huntingtin appears to cure mice (189).

Anticipation is an interesting phenomenon that occurs in HD and other diseases of trinucleotide expansion passed through generations (190). Anticipation is an earlier age of disease onset, with more rapid disease progression in successive generations of a family. As the onset of disease is strongly dependent on the length of triplet repeat, there is a lengthening of the trinucleotide tract within successive generations: thus, there must exist a molecular mechanism of trinucleotide instability.

The current models predict that trinucleotide expansion occurs either during DNA replication or during DNA repair and recombination (191). Slippage of the DNA polymerase during replication has been proposed as a $(CAG/CTG)_n$ tract can form secondary conformation such as stable hairpin structures. It appears that TNR instabilitydepends on orientation: expansion is more likely to occur in the lagging strand (Figure 10). The DNA-repair protein Fen1 is involved in Okazaki fragment processing in the lagging strand (192).

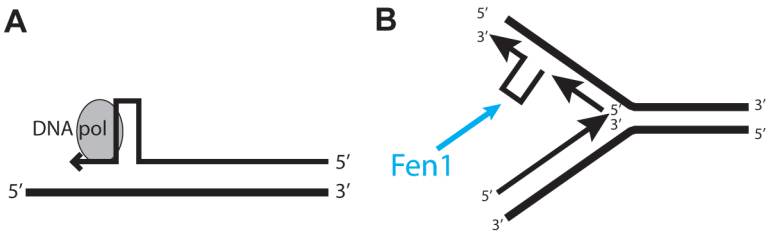

Figure 10: *Models for triplet expansion*. A DNA polymerase slippage during replication. Extrahelical loops are formed due to misalignment of repetitive sequences. The following integration of the tract results in gain of repeat units. B. Expansion during Okazaki fragment processing. Data suggest TNR instability is dependent on orientation, that is, expansion is more likely to occur in the lagging strand. Fen1 is involved in Okazaki fragment processing.

Fen1 deficiency is embryologically lethal (193). Contradictory results have been obtained for mutations in the Fen1 gene regarding its role in trinucleotide expansions. In yeast the loss or haploinsufficiency of Fen1 homologue RAD27 leads to rapid triplet repeat expansion (194, 195). Yeast cells may not be ideal models for TNR instability, as TNRs are not natural elements in their DNA, indicating that mechanisms for repeat maintenance have not been evolutionary conserved (196). In mice, haplo-insufficiency of Fen1 leads to an expansion of CAG-repeats (197). However, with Fen1 haploinsufficiency the stability at a similar locus, myotonic dystrophy type 1 (DM1), appears completely stable (196). In contrast, triplet repeats are unexpectedly stable in the fruit fly *Drosophila Melanogaster,* suggesting that this system may not be suitable for studying repeat instability (198). We have investigated the influence of low levels of the DNA-repair gene Fen1 in human cells, and could not find any effect on the huntingtin triplet repeat locus (5). In human patients, no DNA alterations in the coding region of Fen1 have been found (199). Thus, the mechanisms of triplet repeat instability remain a mystery.

Methodological considerations

Details regarding the different methods are stated in the "Material and methods"-section of the respective papers. However, the following section will expand on some central methods, why we chose them, and work as a basis for the summary of results. Some methods used that have not yet resulted in any publications will also be discussed.

Use of different cell lines
Because much of our work depended on cell lines, the first paragraph gives a short introduction to the use of different cell lines. To study the efficacy of siRNA the classical cell line HeLa was used (1), as it is easily propagated and manipulated. HeLa is short for Henrietta Lachs, a woman who died of aggressive adenocarcinoma of the cervix in 1951 (200). Her cervical biopsy became the first human cancer cell line immortalized in tissue and culture and is today widely used in cell biology. HeLa cells are ideal for studying knockdown of the DNA repair gene Fen1, as Fen1 is endogenously expressed. However, expression of AQP4 had to be introduced by a plasmid, as no non-primary cell lines express the gene.

Although it did not influence our conclusion, the diversity of HeLa cells provided a challenge in examination of the Huntingtin locus in a HeLa derivate named T-REx (5). Density trace plots of the PAGE-gel bands of the huntingtin gene showed a bimodal distribution with a major 16-mer band and a minor 27-mer band. Sequence analysis revealed the same asymmetric bi-modal distribution with predominantly more clones of the 16-mer allele. At first, we suspected that this bias could arise from PCR artifacts, as CAG-repeats theoretically could expand during PCR-amplification (201). However, in a control experiment we showed that our PCR method does not bias the selection of the shorter CAG-tract during amplification. The asymmetry observed by PCR is therefore thought to arise from chromosomal rearrangements within the T-REx cell line.

It could be argued that cervical cancer cells might not contain the appropriate interaction partners of AQP4, and therefore conclusions regarding AQP4 in HeLa cells should be interpreted with caution. As AQP4 is highly expressed in astrocytes *in vivo* (106), the astrocytic cell line CRL2006 was considered a more suitable cell line to study localization of the four new AQP4 isoforms (4). In addition, as a control we replicated our findings of isoform interaction found in HeLa in CRL2006 (Figure S3)(6).

Design of the FenRex cell line
The DNA repair gene Fen1 has been proposed to contribute in expansion of trinucleotide repeats (197). To investigate this, we designed a cell line named FenRex with an inducible expression of a shRNA targeting Fen1 (5). Simply adding or removing tetracycline to the growth medium turns the expression of Fen1 off and on, respectively. The cell line was based on a commercially available HeLa derivate, T-REx (Invitrogen), which constitutively expresses the Tet repressor protein through a CMV promoter (Figure 11). The shRNA was ligated into a plasmid (pENTR/H1/TO; Invitrogen) containing a tetracycline inducible promoter (Figure 11).

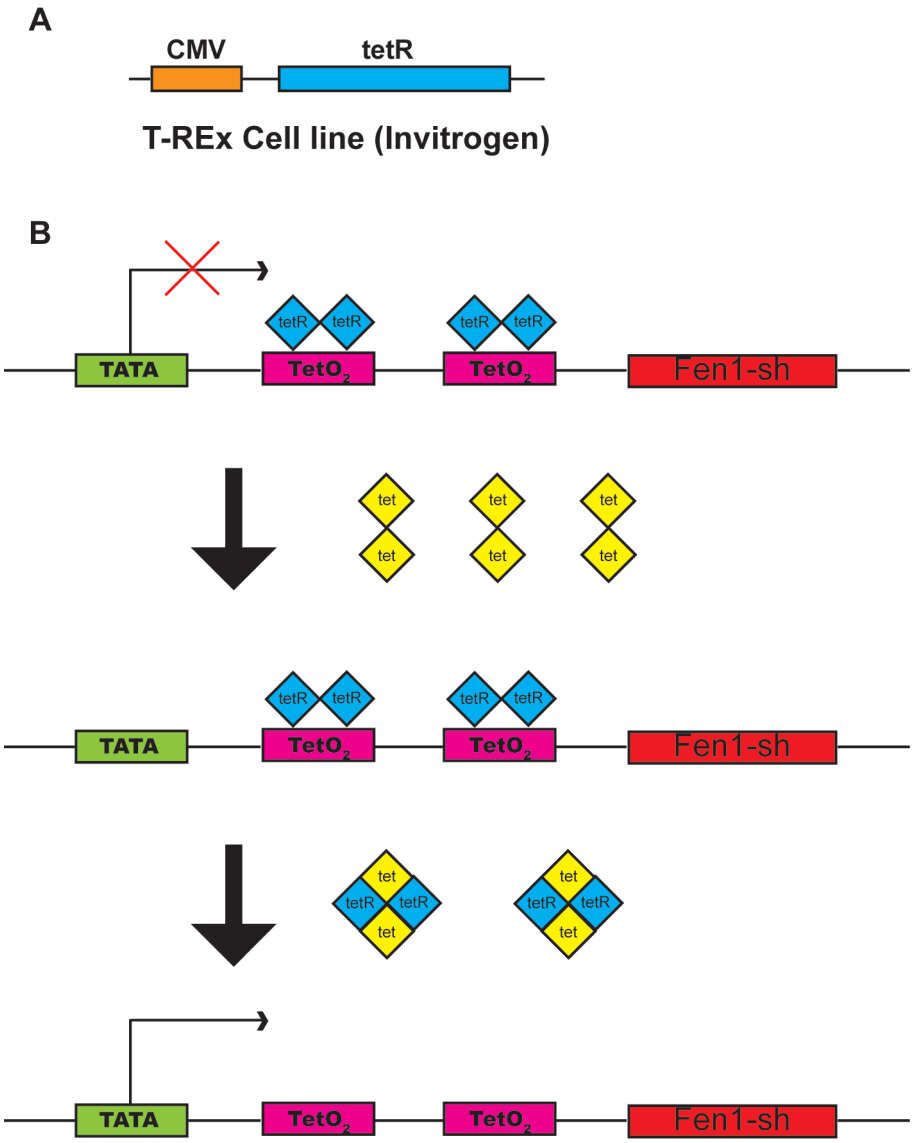

Figure 11: *FenRex cell line.* A. The T-REx cell line from Invitrogen expresses Tet repressor protein (tetR) constitutively through a CMV promoter. B. Upper: In the absence of tetracycline the tetR forms a homodimer with high affinity to the Tet operator sequence (TetO), thereby repressing transcription of the gene of interest (here Fen1-shRNA). Middle/Lower: By adding tetracycline to the medium, the tetracycline will bind the tetR, inducing a conformational change that prevents it from binding TetO and allowing for transcription of the gene.

Dissociated neuronal cultures

We decided to try primary cultures from newborn rat hippocampi as a model system for AQP4, because currently there does not exist any non-primary cells expressing AQP4. After decapitating newborn rats, the brain is isolated and the hippocampus is dissected free and kept on ice. Thereafter the hippocampus is sliced, washed several times in medium before digested with a solution containing trypsin and DNAse. The cells are dissociated through mechanical manipulation, before plated onto to glass cover slips containing extracellular matrix. Within hours neuronal processes will spread out. On the fourth day a nucleoside analogue, cytosine-β-D-arabinofuranoside, is added to the medium to prevent further growth of astrocytes.

This primary cell culture technique was initially successfully applied for detecting AQP4 (2), (Figure 3A), and was also used to downregulate AQP4 using siRNA. However, in later experiments the yield of AQP4 from the hippocampal cultures became fainter, probably as a consequence of a more precise dissection technique. In retrospect one might speculate that the first hippocampal neuronal cultures were contaminated with parts of the brain more abundantly expressing AQP4 in the vicinity of the hippocampus, for instance the habenula or other epithalamic regions, where AQP4 is located in lamellar stacks in high amounts (202). We have also used primary astrocytic cells from neocortex and hippocampal slice cultures, but we have not pursued this.

Plasmid and siRNA transfection

Cell lines are easily transfected with plasmids using liposomes. By means of this method, we have induced transient expression of AQP4 isoforms and evaluated them with Western blotting (2-4, 6). For studying protein expression pattern in the rodent brain, proper controls are essential. We always applied AQP4a and AQP4c transfectants as protein controls when analyzing AQP4 from rat brain specimens.

HeLa cells are also suited for evaluating effects of RNA interference on gene expression. One commonly adapted approach named co-transfection, combines plasmid and siRNA transfection (Figure 12). The co-transfection assay was used to screen 70 siRNAs targeting Fen1 and AQP4 (1). By cloning the coding region of AQP4 or Fen1 cDNA in a reporter construct (pGL3) containing the sequence of firefly luciferase, we were able to express a fusion protein containing luciferase and AQP4 or Fen1. Addition of Dual Luciferase Assay (Promega) provides emission of photons, which can be detected by a luminometer. Co-transfecting the plasmid with gene-specific siRNA is a quick and effective method for evaluating silencing effects, as the siRNA will partly prevent translation of the fusion protein, thereby emitting less light when exposed to the relevant enzymes.

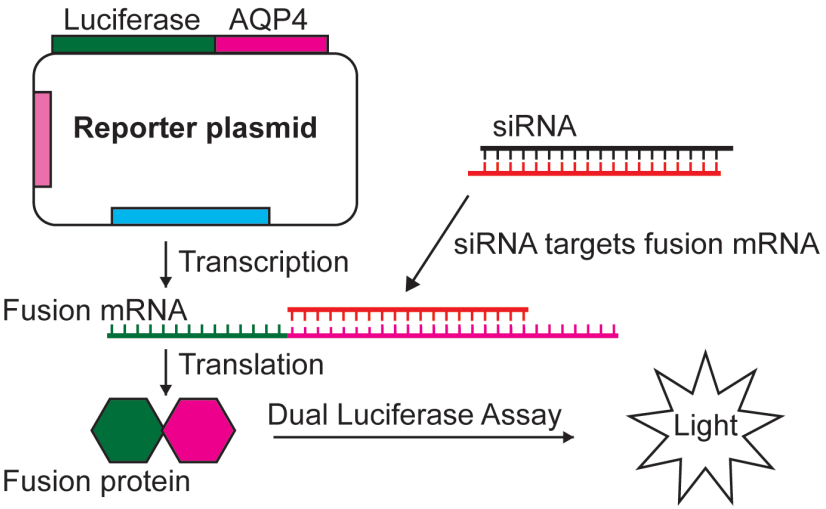

Figure 11: *FenRex cell line.* A. The T-REx cell line from Invitrogen expresses Tet repressor protein (tetR) constitutively through a CMV promoter. B. Upper: In the absence of tetracycline the tetR forms a homodimer with high affinity to the Tet operator sequence (TetO), thereby repressing transcription of the gene of interest (here Fen1-shRNA). Middle/Lower: By adding tetracycline to the medium, the tetracycline will bind the tetR, inducing a conformational change that prevents it from binding TetO and allowing for transcription of the gene.

5'-rapid amplification of cDNA ends (5'RACE) and sequencing
Both bioinformatics and immunoblots indicated that more isoforms might exist (2, 203), although only two isoforms of rat AQP4 was originally known. Mapping of AQP4 from the genomic sequence database against cDNA libraries revealed inconsistencies, and we remapped the 5' end of AQP4 mRNA (4). 5'-*R*apid *A*mplification of *c*DNA *e*nds (5'RACE) is a method for characterizing the 5' end from mRNA using a nested PCR strategy (204). First, a primer including a known sequence oriented towards the 5' end is used in cDNA synthesis. A mix of RNAses degrades the template RNA before the cDNA is purified through a column. Terminal transferase adds a homopolymeric dC-tail to the 3' end of the cDNA. Thereafter, PCR amplification of target cDNA is performed using a second 3'-5'-gene specific primer and an abridged anchor primer, which amplify the dC-tail.

The PCR products were purified from agarose gels and subsequently cloned into pCR2.1-TOPO vector and sequenced. Sequence analysis and alignment were done using the online Basic Local Alignment Search Tool (BLAST) from NCBI. This remapping of the rat genome yielded the discovery of four novel isoforms of rat AQP4 (4). The same technique was used to sequence and analyze 120 PCR-products of the huntingtin gene (5).

TaqMan real-time PCR
To measure siRNA knockdown and mRNA expression patterns, we adapted the method of TaqMan real-time PCR (4, 5). Total RNA was isolated using RNeasy kit (Qiagen). After quantification of total RNA using NanoDrop UV spectrometry, equivalent micrograms of various RNA samples are converted to cDNA by the High Capacity cDNA Archive kit (Applied Biosystems). The use of TaqMan probes against the gene of interest and a suitable reference mRNA, such as GAPDH, β-actin, GFAP or 18S RNA, yields an accurate description of the relative mRNA expression levels of the sample.

TaqMan real-time PCR primers are situated at exon-exon boundaries, thereby controlling for contamination of genomic DNA. The TaqMan probe itself consists of a fluorescent molecule attached to the 5' end and a quencher molecule attached to its 3' end (205). The quencher molecule suppresses the fluorescence emitted when they are located closely to each other. As the Taq polymerase exhibits 5'-3' exonuclease activity, the TaqMan probe is degraded in the amplification process and the fluorescent molecule is released. The fluorescence detected is proportional to the fluorescence released. Hence, the fluorescent signal is proportional to the amount of cDNA in the sample.

Northern blotting
Northern blotting was used for analysis of mRNA knockdown (1). Oligo-$(dT)_n$ Dynabeads (Invitrogen) are used to isolate mRNA from total RNA with subsequent fractionation on a denaturing agarose gel. RNA is blotted overnight to a nylon membrane using high salt solution (206). Blots are labeled using radioactive random priming targeting the coding region of Fen1 or the reference mRNA GAPDH. Radioactive signals are visualized on an imaging plate and scanned. Quantification of relative signal strength between Fen1 and reference protein and comparing it with mock transfections yields the knockdown effect.

Western blotting: SDS-PAGE

Evaluating the amount of AQP4 protein in the brain requires sensitive and reproducible protein immunoblots (207). The use of common lab detergents, such as Triton X-100, CHAPS or deoxycholate, can yield highly erroneous monomer signals, as the AQP4 protein tends to form aggregates during western blotting (2). We screened 55 different detergents with respect to their AQP4 solubilization properties, finding that SDS caused an almost complete breakdown into monomers. Moreover, heating of lysates prior to gel loading (208), collapses the AQP4 signal to a high molecular mass smear. Using the findings of others (203), we showed that inclusion of urea in the resolving gel improved AQP4 monomer resolution. However, the tendency to dimerization of AQP4 remains unclear. Covalent disulfide bridges probably do not cause the dimerization, because addition of the reducing agents β-mercaptoethanol and dithiothreitol do not yield any effects.

The three novel splice variants of AQP4 showed an unusual migration pattern in our SDS-PAGE by appearing at a higher molecular weight than expected (4). It has been shown that polypeptides bind SDS on weight basis (1.4 g SDS/1 g polypeptide) independent of protein sequence (209). The ratio corresponds to an average of one SDS molecule bound for every two amino acids (Figure 13). SDS denatures the proteins native conformation. The negative charge obtained from binding of SDS is much higher than the innate protein charge. Thus, proteins are separated independent of charge by their molecular weight. However, the exon 2-less proteins appear at a higher molecular weight than predicted (4), (Figure 5C). A plausible explanation could be that loss of hydrophobic domains from lacking two transmembrane helices, namely helices 4 and 5, reduced its hydrophobicity. At least in theory, if a protein were less hydrophobic, it would bind less SDS. Less SDS-binding would in turn alter the negative charge of the denatured protein, thereby explaining the unusual migration pattern.

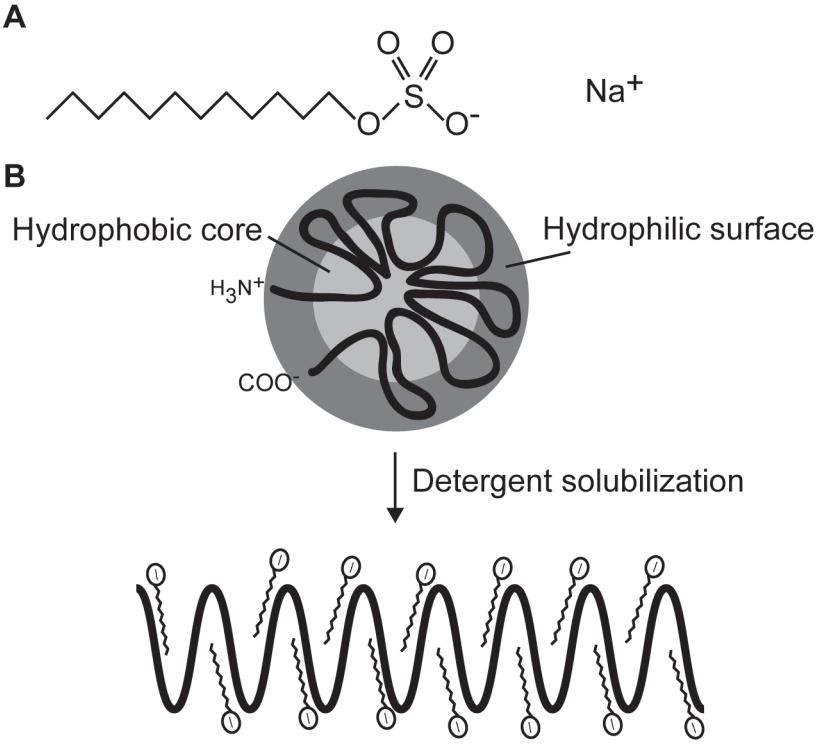

Figure 13: *SDS*. A The structure of Sodium Dodecyl Sulfate (SDS). B. Structure of general cytosolic protein. A protein will have a hydrophobic central core with a hydrophilic surface SDS disrupts non-covalent bonds, resulting in loss of the proteins native conformation. SDS provides negative charge for electrophoretic size separation.

Western blotting: Blue Native PAGE

The native conformations of aquaporins *in vivo* are not monomers, but tetramers (68). In addition, AQP0 and AQP4 are known to form higher order structures as square arrays. To explore the native state of AQP4 in cell membranes, the denaturing SDS-PAGE protocol was insufficient, as SDS dissociates and unfolds proteins. After trying conventional native gel chormotography, which failed, we adapted Blue Native PAGE (BN-PAGE) to investigate the native conformation of AQP4 (210). AQP4a, AQP4e, AQP1 and AQP9 form tetramers, whereas AQP4c and rat brain lysate consist of higher order structures (3). As BN-PAGE requires non-ionic or zwitterionic detergents for solubilization from the lipid bilayer, we chose the mild neutral detergent dodecyl β-D-maltoside (DDM) after calibration experiments (3, 6). For size fractioning proteins must be charged and this is accomplished by the addition of the negatively charged coomassie G-250 dye (211). However, membrane proteins tend to bind large amounts of detergent or coomassie dye, which will add to the protein mass. Thus, the use of molecular size markers tends to overestimate the size of membrane proteins (212). Heuberger *et al.* proposed a factor of 1,8 ± 10% for molecular weight estimation. For instance, the size of an AQP4 monomer is 32 kDa, which provides a tetramer of approximately 130 kDa. In BN-PAGE the tetramer band of AQP4 is located between 242 and 480 kDa. Applying the Heuberger factor, the tetramer of AQP4 should run at 240 ± 24 kDa, indicative of the main band seen on BN-PAGE is representing the tetramer.

We also hypothesized that BN-PAGE could be applied to screen for other candidate genes involved in square array formations. As only C-terminal antibodies are commercially available for AQP4, we had to look elsewhere for the ability to distinguish the various isoforms (4). Simply by adding a C-terminal myc-tail would enable us to differentiate between separate proteins in the higher order structures. We used this to test AQP4 isoform interaction (6). Our method is supported by a later notion that N-terminal GFP-tag has been shown to disrupt higher order molecular structures of AQP4c, whereas a C-terminal reporter-tag does not (213). Our approach could also be applied to test other potential molecular binding partners.

Although BN-PAGE is a rapid and easy assay to complement freeze-fracture in the study of square arrays, there are some limitations. Firstly, as the averaged size of square arrays in astrocytes and AQP4c-transfected cells are 17 IMP and 78 IMP, respectively (114), there is a problem regarding resolution. The highest resolution of higher order bands in BN-PAGE is in the range of 1100 kDa: thus, a maximum of 4-5 IMPs can be observed, assuming one IMP equals one tetramer. Secondly, although DDM is a non-denaturing detergent, it might influence the natural composition of square arrays, as it commonly dissociates labile hydrophobic interactions (214). A clear tetramer band is present in the case of AQP4c, whereas freeze-fracture electron microscopy studies indicate that more than 95% of transfected AQP4c is present as larger assemblies in cell lines (114).

Animal and immunohistochemical studies

All rodent experiments were done according to regulations after an accepted application to the Norwegian Animal Research Authority. Harvesting of material for immunohistochemical staining is achieved by anesthetizing the rodent before perfusing it transcardially with 4% formaldehyde. Analysis of the entire brain and nasal cavity in one section required decalcification by 10% formic acid, as cranium

and teeth could prevent proper sectioning (2). During RNA and protein harvest the animals are anesthetized before decapitation and tissue of interest is dissected and stored in an appropriate medium.

Summary of results

Paper I

Tolerated wobble mutations in siRNAs decrease specificity, but can enhance activity in vivo.

At the moment the siRNA-mediated pathway is still only partially known (53), consequently a better understanding of the basic mechanisms is a major goal. The use of *in vivo* in the title can clearly be misinterpreted, but signals that human cells are used, because most insight in RNA interference has been provided by using cell extracts in a genuine *in vitro* setting. siRNAs exhibit positional effects (28), which means that the efficacy of a siRNA is sensitive to target positions within a given mRNA. Toleration of mutations in siRNA has also been reported, where certain positions within an siRNA are mutated and the siRNA still retains its silencing capacity (29). Design of siRNA is in need of better algorithms for predicting specificity and activity, especially if the target mRNA offers a limited choice of positions. Our aim was to identify siRNA exhibiting efficient and specific silencing against the DNA repair gene Fen1 and the main brain water channel AQP4. The purpose was to identify superior candidates that could be utilized in animal experiments. A total of 70 siRNAs were screened. Initially, the screen evaluated positional effects. We found positional effects in Fen1 and AQP4 mRNA. Several candidates, such as RMC457i, RMC466i, RMC686i compassed very little effect, whereas other siRNAs Fe775i, RMC845i and RAC937i obtained more than 80% silencing capacity and could serve as candidates for future experiments.

We investigated the toleration for mutations by systematically introducing different mutations. A wobble mutation is a base substitution between mRNA and siRNA, where the classical Watson-Crick base pair is replaced by a weaker interaction (Figure 14) (215). We showed that wobble mutations in the central part could cause a pronounced reduction in activity, in accordance with other findings (46). However, mutations in 5'- and 3' ends are well tolerated. Lower binding energy at one end of a siRNA gives better incorporation into the RISC (36, 37). Thus, a prediction would be that wobble mutations should be able to improve silencing capacity. Schwarz *et al*. stated that siRNA designed according to the asymmetry rules would show maximum suppression of target mRNA at concentrations 100-fold lower than other siRNAs (36). Although we did not find this strong effect, we showed that wobble mutations could enhance the activity of a siRNA if directed towards the 5' end.

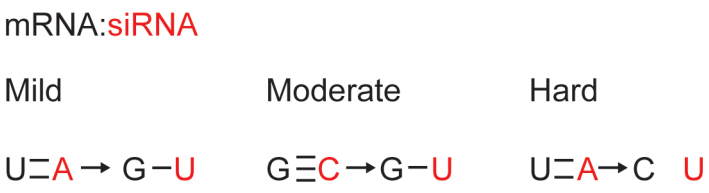

Figure 14: *Wobble mutations*. The effects of mutations in the siRNA sequence; mild, moderate and hard, respectively. A wobble mutation (G:U) can be directed to an A:U pair or a G:C pair. The mild wobble mutation results in loss of one hydrogen bond. Replacing three hydrogen bond G:C pair with a single hydrogen G:U pair results in a moderate mutation. C:U pairs are unable to bind and thus described in this paper as a hard mutation. A C:U pair also disrupts the dsRNA helix.

Paper II

Early upregulation in nasal epithelium and strong expression in olfactory bulb glomeruli suggest a role for Aquaporin-4 in olfaction.

The function of AQP4 in the brain is unknown, although it has been shown that loss of AQP4 protects mice from brain edema in a water intoxication model (119). It has also been suggested that AQP4 plays a role in eclampsia, a condition thought to involve brain edema. The association of AQP4 and eclampsia was reported after AQP4 was found to be 22-fold upregulated during pregnancy (140).

Having established a quantitative and reproducible protocol for APQ4 protein detection, our objective was to test some of the hypotheses regarding the physiological role of AQP4. Because a role for AQP4 in pregnancy-related complications would be important and also shed light on the natural function of AQP4 in the brain, we replicated the experiments of Quick and Cipolla using our optimized and highly sensitive SDS-PAGE. We observed no differences between postpartum and non-pregnant rats. We could not even detect a difference in AQP4 levels between male and female rats.

Another important claim for the natural function for AQP4 is that AQP4 participates in the emptying of fluid from the lungs at birth, as upregulation of AQP4 in lungs at birth was announced (103). However, with use of our sensitive methodology we found no upregulation in lungs at birth. We examined more closely the olfactory system, as a freeze-fracture electron microscopy study (216) and bioinformatic analysis indicated strong AQP4 expression in the nose and the olfactory bulb. We observed a strong AQP4 expression on both sides of the cribriform plate. In the nose AQP4 is upregulated as early as in the brain. We performed immunohistochemistry and found that AQP4 is strongly expressed in the glomerulus. Because the glomerulus is the synaptic unit of the olfactory bulb, we hypothesized that AQP4 could contribute to olfaction. Subsequently, it was reported that $AQP4^{-/-}$ mice have impaired olfaction (158).

Paper III

The molecular compositions of square arrays

The extreme density of square arrays surrounding brain blood vessels is astonishing. Despite the investigation of square arrays by freeze-fracture electron microscopy for more than 40 years the internal organization of square arrays is unknown. Aquaporins in general is known to organize in tetramers (of four monomers). Tetramers of AQP4 can organize into higher order structures known as square arrays (112). Although the composition of square arrays is currently unclear, isoforms have been shown to influence their size (114). Our aim was to investigate the constitution of square arrays. Adapting the technique of Blue Native PAGE, we found that that we could investigate the internal composition of square arrays by biochemical means in a field that so far only had been able to visualize square arrays by freeze-fracture electron microscopy. The rat brain and the isoform AQP4c (M23) was shown to have a range of higher order bands in the BN-PAGE setup. AQP4a (M1), a new isoform AQP4e and two other aquaporins, showed the tetrameric composition. However, combining the BN-PAGE and denaturing gel electrophoresis in a 2D-gel immunoblot on rat brain lysates

showed the compulsory presence of at least three isoforms in each of the higher order bands, indicative of AQP4 being expressed as heteroteramers *in vivo*.

Paper IV

New isoforms of rat Aquaporin-4.

AQP4 was first cloned in rat lung (94), and subsequently two isoforms were found in the rat brain (99). The rat has been the species of choice for studying AQP4 since its discovery. The aim was to investigate AQP4 transcripts in rats based on that protein immunoblotting indicated several isoforms (203), and the fact that a bioinformatics comparison of the rat genome with the rat transcriptome at the AQP4 locus revealed inconsistencies. Hence, we decided to recharacterize the rat AQP4 gene. By use of a 5' RACE screen we discovered the presence of new exons and new splice variants. We found that the rat genome includes 6 isoforms, four of which had not previously been described. Due to the increased complexity, we suggested a simpler nomenclature in line with standards and conventions for gene isoforms, namely AQP4a-f. Three of the new isoforms, lacking exon 2, only include four transmembrane helices. The three exon 2-lacking proteins did not transport water across the cell membrane and no functions of these isoforms have been found. The new longest isoform, named AQP4e, is located in the plasma membrane. It also transports water in a *Xenopus* oocyte water permeability system at a rate comparable with AQP4c (M23).

Paper V

Huntington triplet-repeat locus is stable under long-term Fen1 knockdown in human cells.

The underlying defect in several human neurodegenerative and neuromuscular diseases are expansions of trinucleotide repeats, for instance $(CAG)_n$. Examples of such diseases are Huntington's disease, myotonic dystrophy, fragile X syndrome, spinocerebellar ataxias and Friedrich's ataxia (191). Several hypotheses regarding the mechanisms for trinucleotide expansion exist and can be divided into replication-dependent and repair-dependent. Some models have proposed the DNA-repair Flap Endonuclease 1 (Fen1) to be involved in expansion of trinucleotide repeats. The aim was to investigate the role of Fen1 involvement in genomic instability in human cell lines, by utilizing our best candidate from our previous siRNA screen (1). This also provided the opportunity to get acquainted with DNA-based vectors in RNA interference, which holds a great potential for future *in vivo* experiments.

Fen1 is involved in Okazaki-fragment processing and in repair by removing single-stranded DNA flaps before ligation (192). The involvement of Fen1 in trinucleotide diseases seems to be species dependent, as deletion of Fen1 increases trinucleotide instability in yeast (194), whereas this does not occur in *Drosophila* (198). In mice, haplo-insufficiency of Fen1 has been reported to expand CAG-repeats in the huntingtin gene (197). However, no expansion was seen with Fen1 haplo-insufficiency in a mouse model of Mytonic dystrophy type 1 (196). The role of Fen1 in genomic instability has previously not been investigated in human cells. However, no mutations of Fen1 were found in patients with Huntington's disease (199).

An inducible RNA hairpin vector was designed on the basis of our best candidate directed against Fen1, and the FenRex cell line was created. The cells were observed over 27 successive generations, yielding a 10^{17} expansion of the cell population. As one human includes 10^{13} cells (9), the time course in this study should be sufficient to observe expansion in the repetitive pattern of the huntingtin locus. However, no significant shift in allele length of the Huntington's disease gene was observed by PCR or mRNA-sequencing. Moreover, no significant growth inhibition compared to control cells were observed, suggesting that low levels of Fen1 is sufficient for Okazaki fragment processing. Another finding was that no alteration in the expression levels of Fen1's molecular binding partner PCNA were observed, suggesting that there is no feedback regulation between them. In conclusion, our findings in human cells argue against a role for Fen1 in triggering huntingtin triplet repeat expansion.

Paper VI

Roles of aquaporin-4 isoforms and amino acids in square array assembly.

The size of square arrays is influenced by isoforms, as AQP4a (M1) mostly produces single intramembrane particles, whereas AQP4c (M23) produces huge square lattices (114). Building on our BN-PAGE and our discovery of new AQP4 isoforms, the aim was to investigate the isoform influence on square array assembly and develop a membrane-protein-protein interaction assay.

From the 2D crystallization of AQP4 it was proposed that the basic amino acids in the N-terminal of AQP4a blocks tetramer-tetramer binding sites (149). It was also proposed that five lateral binding sites in AQP4c could account for tetramer-tetramer interaction. We tested this hypothesis by mutating critical amino acids and assaying the effect on higher order structures using BN-PAGE. No alterations in higher order structures were found when mutating the basic amino acids of the AQP4a N-terminal. Not even triple mutations of the proposed lateral tetramer-tetramer binding sites in AQP4c, causing the loss of all five putative interaction sites, did break down the higher order structures. However, through a double mutation of the cysteine C13 and C17 in AQP4a, we observed an incomplete shift into square arrays, as proposed by freeze-fracture electron microscopy (115). We could not detect any influence on square array assembly by mutating putative phosphorylation sites of introducing a stop-codon in the PDZ-domain, a domain proposed be involved in anchoring of AQP4 in the cell membrane (162).

Although several publications have proposed AQP4 molecular binding partners, including components of the endocytosis machinery (217), various kinases and structural proteins in astrocytic endfeet (162), conclusive evidence regarding molecular binding partners is lacking. Contrary to the view of others (203), Crane and Verkman proposed that AQP4a and AQP4c do not coassociate in live cells using quantum dot single particle tracking (218). AQP4a and AQP4e are unable to form higher order structures on their own. Whereas there exist no commercial antibodies available to distinguish the different isoforms, we myc-tagged the C-terminal of AQP4a and AQP4e. Co-transfecting AQP4a-myc and AQP4e-myc with AQP4c incorporated these isoforms into higher order structures. Accordingly, we found an

interaction between isoforms in higher order structures. This provides further evidence that the square arrays are hetero-tetramers of the various isoforms.

Discussion

The most common pharmaceuticals today target proteins. Theoretically, the discovery of RNA interference provides the opportunity to intervene at an even earlier stage, namely at the mRNA level. In the following years it will be exciting to observe if the RNAi medication in clinical trials will change the concept of human drug therapy.

Although drugs utilizing RNAi are in clinical trials, some of the basic properties of RNAi remain unclear (53). A more thorough understanding could allow better algorithms in designing siRNA. We have investigated positional effects, showing that some siRNAs targeting mRNA exhibit very little activity, whereas others show high silencing capacity depending on their position within target mRNA (1). The mechanism for the observed positional effects is currently not fully understood, but the main hypothesis has attributed positional effects to biased strand loading (36, 37).

In biased strand loading, the thermodynamic stability of the 5' end of a siRNA-duplex influences the strand loading. Our findings support this to some degree, in the sense that weakening of interactions at the 5' end through wobble mutations of the antisense strand improves activity. However, if only siRNA-duplex stability in one end is the determinant of RISC loading, one could predict that wobble mutations of the corresponding nucleotide at the 3' end in the sense strand would also improve silencing. However, we could not observe such an effect. Alternatively, positional effects might occur as a consequence of the RISC complex favoring certain secondary mRNA structures (219).

We investigated the effects of mutations in certain positions of the siRNA. Mutations in the central part of the antisense strand caused reduced activity. This is in agreement with earlier investigations, which led to believe that even a single mismatch at the target site could obliterate silencing capacity (27). However, terminal mutations were tolerated. The need for algorithms for improving siRNA, is of crucial importance when the target mRNA offers limited positions.

Examples of such targets are genetic diseases. In dominantly inherited diseases, such as Huntington's disease, the patients are often heterozygous. The $(CAG)_n$ tract does not offer any targets, as a 21 nt siRNA will not be able to distinguish the normal and the pathological allele. Moreover, the normal huntingtin gene appears vital to normal neuronal function, as conditional knockout promotes severe neurodegeneration (220). Nonetheless, studies have identified single nucleotide polymorphisms in patients with Huntington's disease (221). Targeting disease-specific single nucleotide polymorphisms with an effective siRNA could be future therapy for patients with Huntington's disease.

Our results show that triple mutations are not tolerated. This maximum mutation threshold could be a general mechanism for siRNA to avoid off-target effects. Off-target effects create the risk of downregulation of other genes than the target gene. Bioinformatics analysis has shown that triple mutations increase the risk of off-target alignments in 75% of 359 published siRNA sequences (48). Furthermore, we have shown that it is difficult to improve an already superior siRNA by mutations. Our findings of highly effective siRNA candidates against Fen1 and AQP4 could also be advantageous for researchers investigating these genes.

We applied the best candidate from our screen to design a short hairpin RNA against Fen1 (5). By doing so, a human cell line capable of silencing Fen1 protein 10-fold in a regulated fashion was created simply by adding tetracycline to the growth medium. We used this cell line to investigate the involvement of Fen1 in genomic instability. The role of Fen1 in triplet repeat expansion has led to contrasting results in different species. We observed no initiation of trinucleotide expansion of huntingtin $(CAG)_n$ by downregulating Fen1 during 27 successive generations. Although our conclusion does not support a role of Fen1 in initiating triplet repeats, it would be interesting to repeat our study in a cell line already containing a pathological CAG-repeat, as Fen1 might be involved in the anticipation phenomenon observed in patients with Huntington's disease.

Exploring further roles of the DNA-repair gene Fen1 by means of the FenRex cell line is beyond our scope, although all cell passages are still available. It is tempting to speculate whether the cell line could be utilized in future experiments, perhaps within the field of cancer biology. Examples of applications could be the Comet Assay, microarray analysis, time kinetics and immunohistochemistry. Because many studies already have been performed in model organisms, they could easily be replicated in human cell lines.

Originally our principal goal was to use RNAi *in vivo* to downregulate the water channel AQP4 in the rodent brain. This could in theory be a future intervention for brain edema, as lack of AQP4 was proven beneficial in models of hyponatremic brain edema and hemispheric stroke (119). AQP4 may also be the target of NMO-antibodies, implicating AQP4 in the pathophysiology of the demyelinating disease neuromyelitis optica (173). $AQP4^{-/-}$ mice are protected from demyelinating lesions when exposed to NMO-IgG (176). Thus, downregulation of AQP4 in the brain *in vivo* could theoretically induce less tissue damage. Furthermore, developing RNAi as a research tool would help elucidating the unknown role of AQP4 in the brain.

Aquaporins have a well-understood physiological function in the kidney. In each segment, various aquaporins are present, allowing the nephron to function properly. The presence of aquaporins on both apical and basolateral membranes provide a fast transcellular pathway for water. Mutations of AQP1-4 all show some defect in urinary concentration. The role for aquaporins in the mammalian brain is much less understood, but it is believed to be of significant importance. This is emphasized by the abundant expression of AQP4 near the blood-brain barrier in the perivascular end-feet of astrocytes.

It has been estimated that AQP4 to contributes 0.12% of the rat brain protein (222). Moreover, 99.7% of the endothelial tube of brain microvessels have end-feet coverage (223). Although there are many different membrane proteins, AQP4 covers approximately 36% of the astrocytic cell membrane in the end-feet of rats (109). In spite of that, mice lacking AQP4 show no neurological or neuroanatomical deficits (79). Moreover, there is no known need for rapid water transport in the brain. Thus, the role of AQP4 in the brain remains unknown.

In disagreement with current models, we showed that there actually are 6 isoforms of rat AQP4 (4), and we proposed a new nomenclature and a new genomic model of rat

AQP4 organization. We could find no evidence for the proposed transcription start of AQP4c (M23) in exon 1, but we propose a transcription start in the new exon X. Later, exon X was not found in the rat cochlea (224), arguing against a role for our genomic model in rat. However, the same authors also describe exon X in the rat cerebellum. It is therefore tempting to ask if cochlear tissues or the brain are of most relevance to AQP4 biology?

We unraveled three new splice variants lacking exon 2. The loss of exon 2 yields a protein containing only four transmembrane helices, whereas all other aquaporins have 6 transmembrane helices. These novel isoforms are not transported to the cell membrane. Nevertheless, other aquaporins have been found in intracellular compartments (68). We have shown that AQP4d colocalize with a *cis*-Golgi marker, but a role for the aquaporins in the Golgi apparatus, is not known. As a result of intracellular localization and loss of pore structure due to the loss of helices 4 and 5, none of these isoforms transported water in an oocyte water transport assay.

After their discovery the splice variants have not lead to further insight. They have been considered an evolutionary by-product, as their functional significance and localization in the brain is unkown. However, our methodology has been applied to cochlear tissue (224). Consistent with our findings, the exon 2-less transcripts were observed using TaqMan in cochlea, and were estimated to contribute to around 5% of total AQP4 mRNA-transcripts. Another more surprising finding, was an immunolocalization study showing that AQP4d is located in the cell membrane (225). It is difficult to explain the discrepancy between our results, but one hypothesis might be that the GFP-tag used in the latter study somehow influences membrane localization. For instance, it has been shown that N-terminal GFP-AQP4c chimeras disrupt square array formation (226).

Unlike the exon 2-less isoforms, the discovery of the novel isoform AQP4e has attracted notice and led to further insight. AQP4e was unable to form higher order structures on its own (3), but would organize into higher order structures when co-transfected with AQP4c (6). It also is a candidate for the third AQP4 band, named the Mz-band, observed in rat brain lysates on SDS-PAGE (2, 203) and on BN-PAGE (3).

We showed that AQP4e was a functional water channel (4). Subsequently, it has been verified as a functional water channel, being impermeable to smaller osmolytes, and also shown to be unable to organize into square arrays by freeze-fracture electron microscopy (227). Strengthening the observations from freeze-fracture and BN-PAGE, AQP4e did not assemble in square arrays by single molecular tracking (228). Both papers reproduced our BN-PAGE findings of AQP4e (3). We found no evidence of the existence of AQP4e in humans or mice. This is supported by a later publication (228).

Because the TaqMan assay targets exon-exon boundaries, a distinction of the relative mRNA expression of the different isoforms is difficult to obtain. Our results suggest, however, that the exon 2-less transcripts are 20 times less expressed on mRNA level than the isoforms AQP4e, AQP4a and AQP4c. Although quantification of the relative expressions of the different isoforms of AQP4 is limited by the sharing of exons, we observed a discrepancy between mRNA levels and protein levels (4). Relative quantification of proteins has estimated a ratio between AQP4a and AQP4c of

approximately 1:10 (2, 203). Transcripts containing AQP4c, however, are much less abundant than the other isoforms. This discrepancy could be explained if AQP4c is stabilized in square arrays.

Although our results support square arrays being hetero-tetramers *in vivo*, the abundance of AQP4c indicates that it is the major component of square arrays. It is therefore tempting to speculate that AQP4c is the main building block, whereas the other isoforms serves as regulatory end-points in the rafts. It may be argued that huge rafts are more difficult to internalize by endocytosis. Hence, AQP4c is more protected from degradation in the cell membrane. Alternatively, a pathway for endocytosis could be through adaptor proteins binding the N-terminal of AQP4, promoting less degradation of AQP4c.

However, if it turns out that the protein stability is unchanged, there must be another explanation. The observed discrepancy may be due to regulation on the mRNA level. Initiation of translation may occur through a consensus sequence surrounding the start codon (229). Leaky scanning occurs during eukaryotic translation when ribosomes initiate translation from several different start codons. We propose that the observed discrepancy between mRNA and protein levels could be due to leaky scanning during translation. The observation that transfected wild-type AQP4e produces three immunoblot bands, whereas introduction of an optimized Kozak-sequence in AQP4e produces only a single band, is supporting our conclusion (Figure 5) (4). Others have later used the same line of arguments (230).

Although there exists 6 transcripts in the rodent brain, most studies investigate AQP4 at the protein level. The link between AQP4 and square arrays came from the observation that AQP4-deficient mice lacked square arrays (111). AQP4 forms huge rectangular assemblies with sizes ranging up to 2400 nm^2 (109). The abundance of these large rectangular assemblies is puzzling. However, isoforms have been shown to influence their size. Whereas AQP4a only produces tetramers, AQP4c produces large square arrays (114). Combining the two isoforms of AQP4 in the membrane gave a distribution more similar, but not equivalent with regards to shape and size, to the natural distribution in astrocytes. If transfection of cell lines is unable to reconstitute the *in vivo* shape and size of square arrays, there must be some information lacking. We proposed that this could be due to that fact that rat AQP4 contains more isoforms than the two investigated by freeze-fracture electron microscopy. Alternatively, there might be fundamental differences between astrocytes *in vivo* and in cell lines. For instance, there might exist some molecular chaperones in astrocytes responsible for organizing square arrays, or cell lines might lack the appropriate anchoring proteins. Alternatively, there could exist an unknown protein in square arrays.

To investigate the native conformation of AQP4, we adapted the biochemical assay BN-PAGE (3). This was the first approach to observe square arrays by other means than freeze-fracture electron microscopy. Subsequently, another approach using single molecular tracking has been adapted (218). We showed that AQP4 from rodent brain consists of a main tetramer band and several higher order bands. The size of these higher order bands indicated that they could be multiples of AQP4 dimers. The isoform AQP4a was unable to form higher order bands on its own, whereas AQP4c produced multiple higher order bands (6). This was consistent with the observation in freeze-fracture (114). In addition, 2D-gel immunoblotting of rat brain samples

showed each higher order band including at least three AQP4 proteins, indicative of more isoforms being present in square arrays.

As discussed previously there are some limitations to our BN-PAGE setup: especially the size resolution is of concern. It has been shown that large pore BN-PAGE could be used to separate protein complexes up to 10 MDa (231). Large pore gels have been shown to increase AQP4 resolution in BN-PAGE (232). Although the non-denaturing agent DDM is known to dissociate labile hydrophopic interactions (214), we do not believe it precludes meaningful interpretation (233). Neither have we made the argument that BN-PAGE can replace freeze-fracture analysis. We think that "orthogonal" is a morphological property that can only be visualized with the power resolution of an electron microscope (127). However, freeze-fracture electron microscopy is a demanding method limited to few laboratories, whereas everyone can apply the methodology of BN-PAGE. It was therefore somewhat surprising that we received criticism for applying commercially premade gels and buffers (234), as wide adaptability was one of our main intentions when developing this assay for higher order structures of AQP4.

We have utilized BN-PAGE as a fast assay to investigate AQP4 organization (6). We investigated the proposed interactions in tetramer assembly based on the 2D crystallization of AQP4 (149), without observing a breakdown of higher order structures. In agreement with data from single molecular tracking, we also found the proposed model inadequate (226). It was reported that a double mutant of AQP4a (C13A/C17A) could produce square arrays visualized by freeze-fracture (115). In our BN-PAGE the double mutants produced an incomplete shift towards higher order structures, suggesting that they are probably not the only factor. Supportive of this, single molecular tracking has shown that the ability for C13A/C17A to produce square arrays, only occurs at reduced temperature and can also be modulated by membrane concentration (235).

Surprisingly, initial results from the single molecular tracking technique disagreed with our BN-PAGE setup in the fundamental finding of AQP4 being hetero-tetramers of the different isoforms (218). This contrasted the current view in the field (203), and made our results from 2D gel immunoblotting difficult to interpret (3). However, with improvements in the single molecular tracking, a consensus emerged (236). By applying BN-PAGE and co-transfecting AQP4a and AQP4c similar results to ours were obtained. Furthermore, we showed that AQP4e can interact with AQP4c into higher order structures (6). Afterwards, even a mathematical model predicts square arrays indeed being hetero-tetramers of AQP4 isoforms (232).

The regulation of kidney collecting duct water channel AQP2 is a well-established mechanism in response to ADH. However, the regulation of its brain relative AQP4 is not clear. We applied our BN-PAGE to investigate the influence of proposed phosphorylation sites on square array formation (6). In no cases were the square array formation disrupted. More than 2,000 publications on AQP4 have not yet yielded an unambiguous answer to the question of regulation. Thus, it is our current view that AQP4 is probably constitutively expressed in the cell membrane, which is supported in a recent review (237).

The third band of AQP4, the Mz-band, in optimized SDS-PAGE provided us clues that there might exist additional isoforms in rats (203). It has been shown that Mz actually is AQP4, but unfortunately the mass spectrometry sequence coverage was too poor to differentiate it further (222). Thus, it is not clear whether this band represents a post-transcriptional modification or it is a separate isoform. The novel transmembrane isoform AQP4e has been proposed to contribute to the third AQP4 band, and today it serves as the main hypothesis in the field. However, by a closer look at Figure 5 in Moe *et al.* AQP4e migrated slightly higher than the observed Mz-band of rat brain (4). Thus, we have not concluded upon AQP4e being the third AQP4 protein in the rat brain.

The purification and mass spectrometry study also revealed a fourth AQP4 band at 38 kDa, which could shed light on the splice isoforms. There might be some post-translational modification of AQP4e in astrocytes *in vivo,* resulting in slower migration during gel electrophoresis. Alternatively, a post-translational modification *in vivo* could remove certain residues, making AQP4e slightly smaller. A third possibility is the existence of another exon located upstream. We have no evidence of any modification, nor have we found other exons.

An interesting experiment would be to transfect all three transmembrane isoforms (AQP4e, AQP4a and AQP4c) in a stoichiometric ratio corresponding to the relative protein ratios observed *in vivo*. If the square array distribution in astrocytes can be recreated in cell lines, we could reject hypotheses regarding anchoring proteins, molecular chaperones or an unknown protein X.

Although a role for AQP4 in peripheral tissues is debated, we found a weak but consistent mRNA expression of AQP4 in the heart (4). This finding has been further explored, showing that AQP4 is expressed in myocardial cells at low levels, and proposed to participate during ischemic injury (238).

We found an early upregulation of AQP4 in the nasal mucosa (2), similar to the early upregulation in the brain. Immunohistochemistry showed a strong labeling in the respiratory epithelium, where a potential role of AQP4 could be helping to humidify the air entering the lungs. We also found strong labeling in the olfactory glands of Bowman and in basal cells. *In situ* hybridization shows that basal cells do not express AQP4: thus, the staining in the basal cell layer is attributed to AQP4 anchored in the basal lamina end-feet of the sustenticular cells (Holen T., unpublished results). Moreover, strong labeling of the glomerular layer of the olfactory bulb was found. Upon these findings we proposed a role for AQP4 in olfaction.

Subsequently, it was reported that $AQP4^{-/-}$ mice had impaired olfaction (158). $AQP4^{-/-}$ mice were slower in finding a buried food pellet and in finding food pellets in an olfactory labyrinth. Furthermore, the mice showed reduced odorant field potentials in an electro-olfactogram, but not complete anosmia. Similar results have been obtained from other sense organs, suggestive of a role for AQP4 in neurotransduction. It has been proposed that its role in neurotransduction involves altered potassium kinetics (161).

Olfaction has long been an underappreciated chemical sense in neuroscience, thought to play a minor role in human biology. However, by the discovery of olfactory

odorant receptors (239), and the following characterization of the olfactory system have inspired researchers. Linda Buck and Richard Axel received the Nobel Prize in Medicine 2004 for their discoveries. Building on our finding in the nose, a more thorough electron microscopy investigation of olfactory mucosa led to the discovery of aquaporin pathways in the olfactory glands (240). AQP4 is expressed at the basolateral sides of acinar cells, whereas AQP5 is present apically: thus, a transcellular water pathway exists. It may be speculated that these pathways play a major role in protection of the olfactory epithelium through hydration. But even more intriguing, they might be important for olfaction, as it could prevent saturation of odorant receptors within the olfactory mucosa, due to the fact that olfactory epithelium lacks motile cilia and the mucociliary clearance. The fluid flux through olfactory glands might also defend against infections by pushing old mucus onto respiratory epithelium, which does have mucociliary clearance.

AQP4 has become the molecular marker of the demyelinating disease neuromyelitis optica (173). If AQP4 plays role in development of this disease - NMO being an autoantibody-mediated disease- *in vivo* knockdown of AQP4 might be beneficial for these patients. In addition, 53% of patients with disease within the neuromyelitis optica spectrum had olfactory dysfunction, apparently in correlation with AQP4 autoantibodies (241). Based on the immunolocalization of AQP4 to the olfactory system and the high antibody titer in the peripheral blood of NMO patients, we would expect the prevalence to be even higher. However, as awareness of olfactory dysfunction in these patients now is raised, it is tempting to speculate that olfactory dysfunction in the future will be a hallmark of the disease and perhaps even incorporated in new revisions of diagnostic criteria.

In conclusion, our published results have stood the test of time. Some results have been replicated and reproduced, strengthening some of our basic conclusions concerning both RNA interference and AQP4. Although clinical benefits of our work is still uncertain, we have gained knowledge throughout the process and hopefully made a small contribution to the vast field of science.

References

1. Holen T, Moe SE, Sorbo JG, Meza TJ, Ottersen OP, Klungland A. Tolerated wobble mutations in siRNAs decrease specificity, but can enhance activity in vivo. Nucleic Acids Res. 2005;33(15):4704-10.
2. Sorbo JG, Moe SE, Holen T. Early upregulation in nasal epithelium and strong expression in olfactory bulb glomeruli suggest a role for Aquaporin-4 in olfaction. FEBS Lett. 2007;581(25):4884-90.
3. Sorbo JG, Moe SE, Ottersen OP, Holen T. The molecular composition of square arrays. Biochemistry. 2008;47(8):2631-7.
4. Moe SE, Sorbo JG, Sogaard R, Zeuthen T, Petter Ottersen O, Holen T. New isoforms of rat Aquaporin-4. Genomics. 2008;91(4):367-77.
5. Moe SE, Sorbo JG, Holen T. Huntingtin triplet-repeat locus is stable under long-term Fen1 knockdown in human cells. J Neurosci Methods. 2008;171(2):233-8.
6. Strand L, Moe SE, Solbu TT, Vaadal M, Holen T. Roles of aquaporin-4 isoforms and amino acids in square array assembly. Biochemistry. 2009;48(25):5785-93.
7. Crick F. Central dogma of molecular biology. Nature. 1970;227(5258):561-3.
8. Mazzarello P. A unifying concept: the history of cell theory. Nat Cell Biol. 1999;1(1):E13-5.
9. Bianconi E, Piovesan A, Facchin F, Beraudi A, Casadei R, Frabetti F, et al. An estimation of the number of cells in the human body. Ann Hum Biol. 2013;40(6):463-71.
10. Crick FH. On protein synthesis. Symp Soc Exp Biol. 1958;12:138-63.
11. Lander ES, Linton LM, Birren B, Nusbaum C, Zody MC, Baldwin J, et al. Initial sequencing and analysis of the human genome. Nature. 2001;409(6822):860-921.
12. Venter JC, Adams MD, Myers EW, Li PW, Mural RJ, Sutton GG, et al. The sequence of the human genome. Science. 2001;291(5507):1304-51.
13. Forbes RM, Cooper AR, Mitchell HH. The composition of the adult human body as determined by chemical analysis. J Biol Chem. 1953;203(1):359-66.
14. Bobbin ML, Rossi JJ. RNA Interference (RNAi)-Based Therapeutics: Delivering on the Promise? Annu Rev Pharmacol Toxicol. 2016;56:103-22.
15. Cerutti H, Casas-Mollano JA. On the origin and functions of RNA-mediated silencing: from protists to man. Curr Genet. 2006;50(2):81-99.
16. Bartel DP. MicroRNAs: genomics, biogenesis, mechanism, and function. Cell. 2004;116(2):281-97.
17. Bernstein E, Kim SY, Carmell MA, Murchison EP, Alcorn H, Li MZ, et al. Dicer is essential for mouse development. Nat Genet. 2003;35(3):215-7.
18. Liu J, Carmell MA, Rivas FV, Marsden CG, Thomson JM, Song JJ, et al. Argonaute2 is the catalytic engine of mammalian RNAi. Science. 2004;305(5689):1437-41.
19. Napoli C, Lemieux C, Jorgensen R. Introduction of a Chimeric Chalcone Synthase Gene into Petunia Results in Reversible Co-Suppression of Homologous Genes in trans. Plant Cell. 1990;2(4):279-89.
20. Hamilton AJ, Baulcombe DC. A species of small antisense RNA in posttranscriptional gene silencing in plants. Science. 1999;286(5441):950-2.
21. Fire A, Xu S, Montgomery MK, Kostas SA, Driver SE, Mello CC. Potent and specific genetic interference by double-stranded RNA in Caenorhabditis elegans. Nature. 1998;391(6669):806-11.
22. Zamore PD. RNA interference: listening to the sound of silence. Nat Struct Biol. 2001;8(9):746-50.
23. Hammond SM, Bernstein E, Beach D, Hannon GJ. An RNA-directed nuclease mediates post-transcriptional gene silencing in Drosophila cells. Nature. 2000;404(6775):293-6.
24. Zamore PD, Tuschl T, Sharp PA, Bartel DP. RNAi: double-stranded RNA directs the ATP-dependent cleavage of mRNA at 21 to 23 nucleotide intervals. Cell. 2000;101(1):25-33.
25. Bernstein E, Caudy AA, Hammond SM, Hannon GJ. Role for a bidentate ribonuclease in the initiation step of RNA interference. Nature. 2001;409(6818):363-6.
26. Stark GR, Kerr IM, Williams BR, Silverman RH, Schreiber RD. How cells respond to interferons. Annu Rev Biochem. 1998;67:227-64.
27. Elbashir SM, Harborth J, Lendeckel W, Yalcin A, Weber K, Tuschl T. Duplexes of 21-nucleotide RNAs mediate RNA interference in cultured mammalian cells. Nature. 2001;411(6836):494-8.

28. Holen T, Amarzguioui M, Wiiger MT, Babaie E, Prydz H. Positional effects of short interfering RNAs targeting the human coagulation trigger Tissue Factor. Nucleic Acids Res. 2002;30(8):1757-66.
29. Amarzguioui M, Holen T, Babaie E, Prydz H. Tolerance for mutations and chemical modifications in a siRNA. Nucleic Acids Res. 2003;31(2):589-95.
30. Rana TM. Illuminating the silence: understanding the structure and function of small RNAs. Nat Rev Mol Cell Biol. 2007;8(1):23-36.
31. Lim LP, Lau NC, Garrett-Engele P, Grimson A, Schelter JM, Castle J, et al. Microarray analysis shows that some microRNAs downregulate large numbers of target mRNAs. Nature. 2005;433(7027):769-73.
32. Bartel DP. MicroRNAs: target recognition and regulatory functions. Cell. 2009;136(2):215-33.
33. Lewis BP, Burge CB, Bartel DP. Conserved seed pairing, often flanked by adenosines, indicates that thousands of human genes are microRNA targets. Cell. 2005;120(1):15-20.
34. Matranga C, Zamore PD. Small silencing RNAs. Curr Biol. 2007;17(18):R789-93.
35. Paddison PJ, Caudy AA, Bernstein E, Hannon GJ, Conklin DS. Short hairpin RNAs (shRNAs) induce sequence-specific silencing in mammalian cells. Genes Dev. 2002;16(8):948-58.
36. Schwarz DS, Hutvagner G, Du T, Xu Z, Aronin N, Zamore PD. Asymmetry in the assembly of the RNAi enzyme complex. Cell. 2003;115(2):199-208.
37. Khvorova A, Reynolds A, Jayasena SD. Functional siRNAs and miRNAs exhibit strand bias. Cell. 2003;115(2):209-16.
38. Haley B, Zamore PD. Kinetic analysis of the RNAi enzyme complex. Nat Struct Mol Biol. 2004;11(7):599-606.
39. Matranga C, Tomari Y, Shin C, Bartel DP, Zamore PD. Passenger-strand cleavage facilitates assembly of siRNA into Ago2-containing RNAi enzyme complexes. Cell. 2005;123(4):607-20.
40. Meister G, Landthaler M, Patkaniowska A, Dorsett Y, Teng G, Tuschl T. Human Argonaute2 mediates RNA cleavage targeted by miRNAs and siRNAs. Mol Cell. 2004;15(2):185-97.
41. Lingel A, Simon B, Izaurralde E, Sattler M. Nucleic acid 3'-end recognition by the Argonaute2 PAZ domain. Nat Struct Mol Biol. 2004;11(6):576-7.
42. Rivas FV, Tolia NH, Song JJ, Aragon JP, Liu J, Hannon GJ, et al. Purified Argonaute2 and an siRNA form recombinant human RISC. Nat Struct Mol Biol. 2005;12(4):340-9.
43. Orban TI, Izaurralde E. Decay of mRNAs targeted by RISC requires XRN1, the Ski complex, and the exosome. RNA. 2005;11(4):459-69.
44. Houseley J, Tollervey D. The many pathways of RNA degradation. Cell. 2009;136(4):763-76.
45. Pei Y, Tuschl T. On the art of identifying effective and specific siRNAs. Nat Methods. 2006;3(9):670-6.
46. Du Q, Thonberg H, Wang J, Wahlestedt C, Liang Z. A systematic analysis of the silencing effects of an active siRNA at all single-nucleotide mismatched target sites. Nucleic Acids Res. 2005;33(5):1671-7.
47. Schubert S, Grunweller A, Erdmann VA, Kurreck J. Local RNA target structure influences siRNA efficacy: systematic analysis of intentionally designed binding regions. J Mol Biol. 2005;348(4):883-93.
48. Snove O, Jr., Holen T. Many commonly used siRNAs risk off-target activity. Biochem Biophys Res Commun. 2004;319(1):256-63.
49. Jackson AL, Bartz SR, Schelter J, Kobayashi SV, Burchard J, Mao M, et al. Expression profiling reveals off-target gene regulation by RNAi. Nat Biotechnol. 2003;21(6):635-7.
50. Semizarov D, Frost L, Sarthy A, Kroeger P, Halbert DN, Fesik SW. Specificity of short interfering RNA determined through gene expression signatures. Proc Natl Acad Sci U S A. 2003;100(11):6347-52.
51. Jackson AL, Linsley PS. Recognizing and avoiding siRNA off-target effects for target identification and therapeutic application. Nat Rev Drug Discov. 2010;9(1):57-67.
52. Bitko V, Musiyenko A, Shulyayeva O, Barik S. Inhibition of respiratory viruses by nasally administered siRNA. Nat Med. 2005;11(1):50-5.
53. Castanotto D, Rossi JJ. The promises and pitfalls of RNA-interference-based therapeutics. Nature. 2009;457(7228):426-33.
54. Kleinman ME, Yamada K, Takeda A, Chandrasekaran V, Nozaki M, Baffi JZ, et al. Sequence- and target-independent angiogenesis suppression by siRNA via TLR3. Nature. 2008;452(7187):591-7.
55. Palliser D, Chowdhury D, Wang QY, Lee SJ, Bronson RT, Knipe DM, et al. An siRNA-based microbicide protects mice from lethal herpes simplex virus 2 infection. Nature. 2006;439(7072):89-94.

56. Soutschek J, Akinc A, Bramlage B, Charisse K, Constien R, Donoghue M, et al. Therapeutic silencing of an endogenous gene by systemic administration of modified siRNAs. Nature. 2004;432(7014):173-8.
57. Zimmermann TS, Lee AC, Akinc A, Bramlage B, Bumcrot D, Fedoruk MN, et al. RNAi-mediated gene silencing in non-human primates. Nature. 2006;441(7089):111-4.
58. Frank-Kamenetsky M, Grefhorst A, Anderson NN, Racie TS, Bramlage B, Akinc A, et al. Therapeutic RNAi targeting PCSK9 acutely lowers plasma cholesterol in rodents and LDL cholesterol in nonhuman primates. Proc Natl Acad Sci U S A. 2008;105(33):11915-20.
59. Fitzgerald K, White S, Borodovsky A, Bettencourt BR, Strahs A, Clausen V, et al. A Highly Durable RNAi Therapeutic Inhibitor of PCSK9. N Engl J Med. 2017;376(1):41-51.
60. Paganelli CV, Solomon AK. The rate of exchange of tritiated water across the human red cell membrane. J Gen Physiol. 1957;41(2):259-77.
61. Macey RI, Farmer RE. Inhibition of water and solute permeability in human red cells. Biochim Biophys Acta. 1970;211(1):104-6.
62. Denker BM, Smith BL, Kuhajda FP, Agre P. Identification, purification, and partial characterization of a novel Mr 28,000 integral membrane protein from erythrocytes and renal tubules. J Biol Chem. 1988;263(30):15634-42.
63. Preston GM, Agre P. Isolation of the cDNA for erythrocyte integral membrane protein of 28 kilodaltons: member of an ancient channel family. Proc Natl Acad Sci U S A. 1991;88(24):11110-4.
64. Preston GM, Carroll TP, Guggino WB, Agre P. Appearance of water channels in Xenopus oocytes expressing red cell CHIP28 protein. Science. 1992;256(5055):385-7.
65. Jung JS, Preston GM, Smith BL, Guggino WB, Agre P. Molecular structure of the water channel through aquaporin CHIP. The hourglass model. J Biol Chem. 1994;269(20):14648-54.
66. Agre P, Sasaki S, Chrispeels MJ. Aquaporins: a family of water channel proteins. Am J Physiol. 1993;265(3 Pt 2):F461.
67. Verkman AS. Aquaporins in clinical medicine. Annu Rev Med. 2012;63:303-16.
68. King LS, Kozono D, Agre P. From structure to disease: the evolving tale of aquaporin biology. Nat Rev Mol Cell Biol. 2004;5(9):687-98.
69. Meinild AK, Klaerke DA, Zeuthen T. Bidirectional water fluxes and specificity for small hydrophilic molecules in aquaporins 0-5. J Biol Chem. 1998;273(49):32446-51.
70. Smith BL, Agre P. Erythrocyte Mr 28,000 transmembrane protein exists as a multisubunit oligomer similar to channel proteins. J Biol Chem. 1991;266(10):6407-15.
71. Ishibashi K, Kondo S, Hara S, Morishita Y. The evolutionary aspects of aquaporin family. Am J Physiol Regul Integr Comp Physiol. 2011;300(3):R566-76.
72. Ma T, Song Y, Gillespie A, Carlson EJ, Epstein CJ, Verkman AS. Defective secretion of saliva in transgenic mice lacking aquaporin-5 water channels. J Biol Chem. 1999;274(29):20071-4.
73. Hara M, Ma T, Verkman AS. Selectively reduced glycerol in skin of aquaporin-3-deficient mice may account for impaired skin hydration, elasticity, and barrier recovery. J Biol Chem. 2002;277(48):46616-21.
74. Hibuse T, Maeda N, Funahashi T, Yamamoto K, Nagasawa A, Mizunoya W, et al. Aquaporin 7 deficiency is associated with development of obesity through activation of adipose glycerol kinase. Proc Natl Acad Sci U S A. 2005;102(31):10993-8.
75. Ishibashi K, Hara S, Kondo S. Aquaporin water channels in mammals. Clin Exp Nephrol. 2009;13(2):107-17.
76. Kitchen P, Day RE, Salman MM, Conner MT, Bill RM, Conner AC. Beyond water homeostasis: Diverse functional roles of mammalian aquaporins. Biochim Biophys Acta. 2015;1850(12):2410-21.
77. Moore RA. The total number of glomeruli in the normal human kidney. Anat Rec. 1931;48(1):153-68.
78. Ma T, Yang B, Gillespie A, Carlson EJ, Epstein CJ, Verkman AS. Severely impaired urinary concentrating ability in transgenic mice lacking aquaporin-1 water channels. J Biol Chem. 1998;273(8):4296-9.
79. Ma T, Yang B, Gillespie A, Carlson EJ, Epstein CJ, Verkman AS. Generation and phenotype of a transgenic knockout mouse lacking the mercurial-insensitive water channel aquaporin-4. J Clin Invest. 1997;100(5):957-62.
80. Yang B, Gillespie A, Carlson EJ, Epstein CJ, Verkman AS. Neonatal mortality in an aquaporin-2 knock-in mouse model of recessive nephrogenic diabetes insipidus. J Biol Chem. 2001;276(4):2775-9.
81. Ma T, Song Y, Yang B, Gillespie A, Carlson EJ, Epstein CJ, et al. Nephrogenic diabetes insipidus in mice lacking aquaporin-3 water channels. Proc Natl Acad Sci U S A. 2000;97(8):4386-91.

82. Nielsen S, Smith BL, Christensen EI, Knepper MA, Agre P. CHIP28 water channels are localized in constitutively water-permeable segments of the nephron. J Cell Biol. 1993;120(2):371-83.
83. Nielsen S, Pallone T, Smith BL, Christensen EI, Agre P, Maunsbach AB. Aquaporin-1 water channels in short and long loop descending thin limbs and in descending vasa recta in rat kidney. Am J Physiol. 1995;268(6 Pt 2):F1023-37.
84. Preston GM, Smith BL, Zeidel ML, Moulds JJ, Agre P. Mutations in aquaporin-1 in phenotypically normal humans without functional CHIP water channels. Science. 1994;265(5178):1585-7.
85. King LS, Choi M, Fernandez PC, Cartron JP, Agre P. Defective urinary-concentrating ability due to a complete deficiency of aquaporin-1. N Engl J Med. 2001;345(3):175-9.
86. Nielsen S, Frokiaer J, Marples D, Kwon TH, Agre P, Knepper MA. Aquaporins in the kidney: from molecules to medicine. Physiol Rev. 2002;82(1):205-44.
87. Nielsen S, Chou CL, Marples D, Christensen EI, Kishore BK, Knepper MA. Vasopressin increases water permeability of kidney collecting duct by inducing translocation of aquaporin-CD water channels to plasma membrane. Proc Natl Acad Sci U S A. 1995;92(4):1013-7.
88. Brown D, Katsura T, Gustafson CE. Cellular mechanisms of aquaporin trafficking. Am J Physiol. 1998;275(3 Pt 2):F328-31.
89. Rosenthal W, Seibold A, Antaramian A, Lonergan M, Arthus MF, Hendy GN, et al. Molecular identification of the gene responsible for congenital nephrogenic diabetes insipidus. Nature. 1992;359(6392):233-5.
90. Deen PM, Verdijk MA, Knoers NV, Wieringa B, Monnens LA, van Os CH, et al. Requirement of human renal water channel aquaporin-2 for vasopressin-dependent concentration of urine. Science. 1994;264(5155):92-5.
91. Huang Y, Tracy R, Walsberg GE, Makkinje A, Fang P, Brown D, et al. Absence of aquaporin-4 water channels from kidneys of the desert rodent Dipodomys merriami merriami. Am J Physiol Renal Physiol. 2001;280(5):F794-802.
92. Nielsen S, Smith BL, Christensen EI, Agre P. Distribution of the aquaporin CHIP in secretory and resorptive epithelia and capillary endothelia. Proc Natl Acad Sci U S A. 1993;90(15):7275-9.
93. Nielsen S, Nagelhus EA, Amiry-Moghaddam M, Bourque C, Agre P, Ottersen OP. Specialized membrane domains for water transport in glial cells: high-resolution immunogold cytochemistry of aquaporin-4 in rat brain. J Neurosci. 1997;17(1):171-80.
94. Hasegawa H, Ma T, Skach W, Matthay MA, Verkman AS. Molecular cloning of a mercurial-insensitive water channel expressed in selected water-transporting tissues. J Biol Chem. 1994;269(8):5497-500.
95. Oshio K, Watanabe H, Song Y, Verkman AS, Manley GT. Reduced cerebrospinal fluid production and intracranial pressure in mice lacking choroid plexus water channel Aquaporin-1. FASEB J. 2005;19(1):76-8.
96. Amiry-Moghaddam M, Lindland H, Zelenin S, Roberg BA, Gundersen BB, Petersen P, et al. Brain mitochondria contain aquaporin water channels: evidence for the expression of a short AQP9 isoform in the inner mitochondrial membrane. FASEB J. 2005;19(11):1459-67.
97. Yang B, Zhao D, Verkman AS. Evidence against functionally significant aquaporin expression in mitochondria. J Biol Chem. 2006;281(24):16202-6.
98. Yang B, Verkman AS. Water and glycerol permeabilities of aquaporins 1-5 and MIP determined quantitatively by expression of epitope-tagged constructs in Xenopus oocytes. J Biol Chem. 1997;272(26):16140-6.
99. Jung JS, Bhat RV, Preston GM, Guggino WB, Baraban JM, Agre P. Molecular characterization of an aquaporin cDNA from brain: candidate osmoreceptor and regulator of water balance. Proc Natl Acad Sci U S A. 1994;91(26):13052-6.
100. Yang B, Ma T, Verkman AS. cDNA cloning, gene organization, and chromosomal localization of a human mercurial insensitive water channel. Evidence for distinct transcriptional units. J Biol Chem. 1995;270(39):22907-13.
101. Frigeri A, Gropper MA, Turck CW, Verkman AS. Immunolocalization of the mercurial-insensitive water channel and glycerol intrinsic protein in epithelial cell plasma membranes. Proc Natl Acad Sci U S A. 1995;92(10):4328-31.
102. Frigeri A, Gropper MA, Umenishi F, Kawashima M, Brown D, Verkman AS. Localization of MIWC and GLIP water channel homologs in neuromuscular, epithelial and glandular tissues. J Cell Sci. 1995;108 (Pt 9):2993-3002.
103. King LS, Nielsen S, Agre P. Aquaporins in complex tissues. I. Developmental patterns in respiratory and glandular tissues of rat. Am J Physiol. 1997;273(5 Pt 1):C1541-8.

104. Yang B, Verbavatz JM, Song Y, Vetrivel L, Manley G, Kao WM, et al. Skeletal muscle function and water permeability in aquaporin-4 deficient mice. Am J Physiol Cell Physiol. 2000;278(6):C1108-15.
105. Ablimit A, Matsuzaki T, Tajika Y, Aoki T, Hagiwara H, Takata K. Immunolocalization of water channel aquaporins in the nasal olfactory mucosa. Arch Histol Cytol. 2006;69(1):1-12.
106. Wolburg H. Orthogonal arrays of intramembranous particles: a review with special reference to astrocytes. J Hirnforsch. 1995;36(2):239-58.
107. Dermietzel R. Visualization by freeze-fracturing of regular structures in glial cell membranes. Naturwissenschaften. 1973;60(4):208.
108. Landis DM, Reese TS. Arrays of particles in freeze-fractured astrocytic membranes. J Cell Biol. 1974;60(1):316-20.
109. Anders JJ, Brightman MW. Assemblies of particles in the cell membranes of developing, mature and reactive astrocytes. J Neurocytol. 1979;8(6):777-95.
110. Landis DM, Reese TS. Astrocyte membrane structure: changes after circulatory arrest. J Cell Biol. 1981;88(3):660-3.
111. Verbavatz JM, Ma T, Gobin R, Verkman AS. Absence of orthogonal arrays in kidney, brain and muscle from transgenic knockout mice lacking water channel aquaporin-4. J Cell Sci. 1997;110 (Pt 22):2855-60.
112. van Hoek AN, Yang B, Kirmiz S, Brown D. Freeze-fracture analysis of plasma membranes of CHO cells stably expressing aquaporins 1-5. J Membr Biol. 1998;165(3):243-54.
113. Rash JE, Yasumura T, Hudson CS, Agre P, Nielsen S. Direct immunogold labeling of aquaporin-4 in square arrays of astrocyte and ependymocyte plasma membranes in rat brain and spinal cord. Proc Natl Acad Sci U S A. 1998;95(20):11981-6.
114. Furman CS, Gorelick-Feldman DA, Davidson KG, Yasumura T, Neely JD, Agre P, et al. Aquaporin-4 square array assembly: opposing actions of M1 and M23 isoforms. Proc Natl Acad Sci U S A. 2003;100(23):13609-14.
115. Suzuki H, Nishikawa K, Hiroaki Y, Fujiyoshi Y. Formation of aquaporin-4 arrays is inhibited by palmitoylation of N-terminal cysteine residues. Biochim Biophys Acta. 2008;1778(4):1181-9.
116. Binder DK, Papadopoulos MC, Haggie PM, Verkman AS. In vivo measurement of brain extracellular space diffusion by cortical surface photobleaching. J Neurosci. 2004;24(37):8049-56.
117. Yao X, Hrabetova S, Nicholson C, Manley GT. Aquaporin-4-deficient mice have increased extracellular space without tortuosity change. J Neurosci. 2008;28(21):5460-4.
118. Zhang H, Verkman AS. Microfiberoptic measurement of extracellular space volume in brain and tumor slices based on fluorescent dye partitioning. Biophys J. 2010;99(4):1284-91.
119. Manley GT, Fujimura M, Ma T, Noshita N, Filiz F, Bollen AW, et al. Aquaporin-4 deletion in mice reduces brain edema after acute water intoxication and ischemic stroke. Nat Med. 2000;6(2):159-63.
120. Papadopoulos MC, Manley GT, Krishna S, Verkman AS. Aquaporin-4 facilitates reabsorption of excess fluid in vasogenic brain edema. FASEB J. 2004;18(11):1291-3.
121. Saadoun S, Tait MJ, Reza A, Davies DC, Bell BA, Verkman AS, et al. AQP4 gene deletion in mice does not alter blood-brain barrier integrity or brain morphology. Neuroscience. 2009;161(3):764-72.
122. Haj-Yasein NN, Vindedal GF, Eilert-Olsen M, Gundersen GA, Skare O, Laake P, et al. Glial-conditional deletion of aquaporin-4 (Aqp4) reduces blood-brain water uptake and confers barrier function on perivascular astrocyte endfeet. Proc Natl Acad Sci U S A. 2011;108(43):17815-20.
123. Zhou J, Kong H, Hua X, Xiao M, Ding J, Hu G. Altered blood-brain barrier integrity in adult aquaporin-4 knockout mice. Neuroreport. 2008;19(1):1-5.
124. Zeng XN, Xie LL, Liang R, Sun XL, Fan Y, Hu G. AQP4 knockout aggravates ischemia/reperfusion injury in mice. CNS Neurosci Ther. 2012;18(5):388-94.
125. Nico B, Frigeri A, Nicchia GP, Corsi P, Ribatti D, Quondamatteo F, et al. Severe alterations of endothelial and glial cells in the blood-brain barrier of dystrophic mdx mice. Glia. 2003;42(3):235-51.
126. Amiry-Moghaddam M, Williamson A, Palomba M, Eid T, de Lanerolle NC, Nagelhus EA, et al. Delayed K+ clearance associated with aquaporin-4 mislocalization: phenotypic defects in brains of alpha-syntrophin-null mice. Proc Natl Acad Sci U S A. 2003;100(23):13615-20.
127. Noell S, Fallier-Becker P, Deutsch U, Mack AF, Wolburg H. Agrin defines polarized distribution of orthogonal arrays of particles in astrocytes. Cell Tissue Res. 2009;337(2):185-95.
128. Klatzo I. Presidental address. Neuropathological aspects of brain edema. J Neuropathol Exp Neurol. 1967;26(1):1-14.

129. Kimelberg HK. Current concepts of brain edema. Review of laboratory investigations. J Neurosurg. 1995;83(6):1051-9.
130. Rabinstein AA. Treatment of cerebral edema. Neurologist. 2006;12(2):59-73.
131. Yang B, Zador Z, Verkman AS. Glial cell aquaporin-4 overexpression in transgenic mice accelerates cytotoxic brain swelling. J Biol Chem. 2008;283(22):15280-6.
132. Yao X, Derugin N, Manley GT, Verkman AS. Reduced brain edema and infarct volume in aquaporin-4 deficient mice after transient focal cerebral ischemia. Neurosci Lett. 2015;584:368-72.
133. Katada R, Akdemir G, Asavapanumas N, Ratelade J, Zhang H, Verkman AS. Greatly improved survival and neuroprotection in aquaporin-4-knockout mice following global cerebral ischemia. FASEB J. 2014;28(2):705-14.
134. Akdemir G, Ratelade J, Asavapanumas N, Verkman AS. Neuroprotective effect of aquaporin-4 deficiency in a mouse model of severe global cerebral ischemia produced by transient 4-vessel occlusion. Neurosci Lett. 2014;574:70-5.
135. Papadopoulos MC, Verkman AS. Aquaporin-4 gene disruption in mice reduces brain swelling and mortality in pneumococcal meningitis. J Biol Chem. 2005;280(14):13906-12.
136. Bloch O, Papadopoulos MC, Manley GT, Verkman AS. Aquaporin-4 gene deletion in mice increases focal edema associated with staphylococcal brain abscess. J Neurochem. 2005;95(1):254-62.
137. Kimura A, Hsu M, Seldin M, Verkman AS, Scharfman HE, Binder DK. Protective role of aquaporin-4 water channels after contusion spinal cord injury. Ann Neurol. 2010;67(6):794-801.
138. Bloch O, Auguste KI, Manley GT, Verkman AS. Accelerated progression of kaolin-induced hydrocephalus in aquaporin-4-deficient mice. J Cereb Blood Flow Metab. 2006;26(12):1527-37.
139. Tait MJ, Saadoun S, Bell BA, Verkman AS, Papadopoulos MC. Increased brain edema in aqp4-null mice in an experimental model of subarachnoid hemorrhage. Neuroscience. 2010;167(1):60-7.
140. Quick AM, Cipolla MJ. Pregnancy-induced up-regulation of aquaporin-4 protein in brain and its role in eclampsia. FASEB J. 2005;19(2):170-5.
141. Wiegman MJ, Bullinger LV, Kohlmeyer MM, Hunter TC, Cipolla MJ. Regional expression of aquaporin 1, 4, and 9 in the brain during pregnancy. Reprod Sci. 2008;15(5):506-16.
142. Saadoun S, Papadopoulos MC, Hara-Chikuma M, Verkman AS. Impairment of angiogenesis and cell migration by targeted aquaporin-1 gene disruption. Nature. 2005;434(7034):786-92.
143. Saadoun S, Papadopoulos MC, Watanabe H, Yan D, Manley GT, Verkman AS. Involvement of aquaporin-4 in astroglial cell migration and glial scar formation. J Cell Sci. 2005;118(Pt 24):5691-8.
144. Auguste KI, Jin S, Uchida K, Yan D, Manley GT, Papadopoulos MC, et al. Greatly impaired migration of implanted aquaporin-4-deficient astroglial cells in mouse brain toward a site of injury. FASEB J. 2007;21(1):108-16.
145. Smith AJ, Jin BJ, Ratelade J, Verkman AS. Aggregation state determines the localization and function of M1- and M23-aquaporin-4 in astrocytes. J Cell Biol. 2014;204(4):559-73.
146. Saadoun S, Papadopoulos MC, Davies DC, Krishna S, Bell BA. Aquaporin-4 expression is increased in oedematous human brain tumours. J Neurol Neurosurg Psychiatry. 2002;72(2):262-5.
147. Saadoun S, Papadopoulos MC, Krishna S. Water transport becomes uncoupled from K+ siphoning in brain contusion, bacterial meningitis, and brain tumours: immunohistochemical case review. J Clin Pathol. 2003;56(12):972-5.
148. Warth A, Simon P, Capper D, Goeppert B, Tabatabai G, Herzog H, et al. Expression pattern of the water channel aquaporin-4 in human gliomas is associated with blood-brain barrier disturbance but not with patient survival. J Neurosci Res. 2007;85(6):1336-46.
149. Hiroaki Y, Tani K, Kamegawa A, Gyobu N, Nishikawa K, Suzuki H, et al. Implications of the aquaporin-4 structure on array formation and cell adhesion. J Mol Biol. 2006;355(4):628-39.
150. Gonen T, Cheng Y, Kistler J, Walz T. Aquaporin-0 membrane junctions form upon proteolytic cleavage. J Mol Biol. 2004;342(4):1337-45.
151. Zhang H, Verkman AS. Evidence against involvement of aquaporin-4 in cell-cell adhesion. J Mol Biol. 2008;382(5):1136-43.
152. Musa-Aziz R, Chen LM, Pelletier MF, Boron WF. Relative CO2/NH3 selectivities of AQP1, AQP4, AQP5, AmtB, and RhAG. Proc Natl Acad Sci U S A. 2009;106(13):5406-11.
153. Wang Y, Tajkhorshid E. Nitric oxide conduction by the brain aquaporin AQP4. Proteins. 2010;78(3):661-70.
154. Thrane AS, Takano T, Rangroo Thrane V, Wang F, Peng W, Ottersen OP, et al. In vivo NADH fluorescence imaging indicates effect of aquaporin-4 deletion on oxygen microdistribution in cortical spreading depression. J Cereb Blood Flow Metab. 2013;33(7):996-9.
155. Fang X, Yang B, Matthay MA, Verkman AS. Evidence against aquaporin-1-dependent CO2 permeability in lung and kidney. J Physiol. 2002;542(Pt 1):63-9.

156. Li J, Patil RV, Verkman AS. Mildly abnormal retinal function in transgenic mice without Muller cell aquaporin-4 water channels. Invest Ophthalmol Vis Sci. 2002;43(2):573-9.
157. Li J, Verkman AS. Impaired hearing in mice lacking aquaporin-4 water channels. J Biol Chem. 2001;276(33):31233-7.
158. Lu DC, Zhang H, Zador Z, Verkman AS. Impaired olfaction in mice lacking aquaporin-4 water channels. FASEB J. 2008;22(9):3216-23.
159. Padmawar P, Yao X, Bloch O, Manley GT, Verkman AS. K+ waves in brain cortex visualized using a long-wavelength K+-sensing fluorescent indicator. Nat Methods. 2005;2(11):825-7.
160. Binder DK, Yao X, Zador Z, Sick TJ, Verkman AS, Manley GT. Increased seizure duration and slowed potassium kinetics in mice lacking aquaporin-4 water channels. Glia. 2006;53(6):631-6.
161. Nagelhus EA, Horio Y, Inanobe A, Fujita A, Haug FM, Nielsen S, et al. Immunogold evidence suggests that coupling of K+ siphoning and water transport in rat retinal Muller cells is mediated by a coenrichment of Kir4.1 and AQP4 in specific membrane domains. Glia. 1999;26(1):47-54.
162. Neely JD, Amiry-Moghaddam M, Ottersen OP, Froehner SC, Agre P, Adams ME. Syntrophin-dependent expression and localization of Aquaporin-4 water channel protein. Proc Natl Acad Sci U S A. 2001;98(24):14108-13.
163. Eid T, Lee TS, Thomas MJ, Amiry-Moghaddam M, Bjornsen LP, Spencer DD, et al. Loss of perivascular aquaporin 4 may underlie deficient water and K+ homeostasis in the human epileptogenic hippocampus. Proc Natl Acad Sci U S A. 2005;102(4):1193-8.
164. Ruiz-Ederra J, Zhang H, Verkman AS. Evidence against functional interaction between aquaporin-4 water channels and Kir4.1 potassium channels in retinal Muller cells. J Biol Chem. 2007;282(30):21866-72.
165. Zhang H, Verkman AS. Aquaporin-4 independent Kir4.1 K+ channel function in brain glial cells. Mol Cell Neurosci. 2008;37(1):1-10.
166. Jin BJ, Zhang H, Binder DK, Verkman AS. Aquaporin-4-dependent K(+) and water transport modeled in brain extracellular space following neuroexcitation. J Gen Physiol. 2013;141(1):119-32.
167. Iliff JJ, Wang M, Liao Y, Plogg BA, Peng W, Gundersen GA, et al. A paravascular pathway facilitates CSF flow through the brain parenchyma and the clearance of interstitial solutes, including amyloid beta. Sci Transl Med. 2012;4(147):147ra11.
168. Xie L, Kang H, Xu Q, Chen MJ, Liao Y, Thiyagarajan M, et al. Sleep drives metabolite clearance from the adult brain. Science. 2013;342(6156):373-7.
169. Takahashi T, Fujihara K, Nakashima I, Misu T, Miyazawa I, Nakamura M, et al. Anti-aquaporin-4 antibody is involved in the pathogenesis of NMO: a study on antibody titre. Brain. 2007;130(Pt 5):1235-43.
170. Wingerchuk DM, Lennon VA, Lucchinetti CF, Pittock SJ, Weinshenker BG. The spectrum of neuromyelitis optica. Lancet Neurol. 2007;6(9):805-15.
171. Lennon VA, Wingerchuk DM, Kryzer TJ, Pittock SJ, Lucchinetti CF, Fujihara K, et al. A serum autoantibody marker of neuromyelitis optica: distinction from multiple sclerosis. Lancet. 2004;364(9451):2106-12.
172. Mader S, Lutterotti A, Di Pauli F, Kuenz B, Schanda K, Aboul-Enein F, et al. Patterns of antibody binding to aquaporin-4 isoforms in neuromyelitis optica. PLoS One. 2010;5(5):e10455.
173. Lennon VA, Kryzer TJ, Pittock SJ, Verkman AS, Hinson SR. IgG marker of optic-spinal multiple sclerosis binds to the aquaporin-4 water channel. J Exp Med. 2005;202(4):473-7.
174. Hinson SR, Pittock SJ, Lucchinetti CF, Roemer SF, Fryer JP, Kryzer TJ, et al. Pathogenic potential of IgG binding to water channel extracellular domain in neuromyelitis optica. Neurology. 2007;69(24):2221-31.
175. Crane JM, Lam C, Rossi A, Gupta T, Bennett JL, Verkman AS. Binding affinity and specificity of neuromyelitis optica autoantibodies to aquaporin-4 M1/M23 isoforms and orthogonal arrays. J Biol Chem. 2011;286(18):16516-24.
176. Saadoun S, Waters P, Bell BA, Vincent A, Verkman AS, Papadopoulos MC. Intra-cerebral injection of neuromyelitis optica immunoglobulin G and human complement produces neuromyelitis optica lesions in mice. Brain. 2010;133(Pt 2):349-61.
177. Rash JE, Davidson KG, Yasumura T, Furman CS. Freeze-fracture and immunogold analysis of aquaporin-4 (AQP4) square arrays, with models of AQP4 lattice assembly. Neuroscience. 2004;129(4):915-34.
178. Lutterotti A, Vedovello M, Reindl M, Ehling R, DiPauli F, Kuenz B, et al. Olfactory threshold is impaired in early, active multiple sclerosis. Mult Scler. 2011;17(8):964-9.
179. DeLuca GC, Joseph A, George J, Yates RL, Hamard M, Hofer M, et al. Olfactory Pathology in Central Nervous System Demyelinating Diseases. Brain Pathol. 2015;25(5):543-51.

180. Schmidt F, Goktas O, Jarius S, Wildemann B, Ruprecht K, Paul F, et al. Olfactory dysfunction in patients with neuromyelitis optica. Mult Scler Int. 2013;2013:654501.
181. Huntington G. On Chorea. Med Surg Rep. 1872;26(15):317-21.
182. A novel gene containing a trinucleotide repeat that is expanded and unstable on Huntington's disease chromosomes. The Huntington's Disease Collaborative Research Group. Cell. 1993;72(6):971-83.
183. Duyao MP, Auerbach AB, Ryan A, Persichetti F, Barnes GT, McNeil SM, et al. Inactivation of the mouse Huntington's disease gene homolog Hdh. Science. 1995;269(5222):407-10.
184. Mangiarini L, Sathasivam K, Seller M, Cozens B, Harper A, Hetherington C, et al. Exon 1 of the HD gene with an expanded CAG repeat is sufficient to cause a progressive neurological phenotype in transgenic mice. Cell. 1996;87(3):493-506.
185. Gu X, Andre VM, Cepeda C, Li SH, Li XJ, Levine MS, et al. Pathological cell-cell interactions are necessary for striatal pathogenesis in a conditional mouse model of Huntington's disease. Mol Neurodegener. 2007;2:8.
186. Davies SW, Turmaine M, Cozens BA, DiFiglia M, Sharp AH, Ross CA, et al. Formation of neuronal intranuclear inclusions underlies the neurological dysfunction in mice transgenic for the HD mutation. Cell. 1997;90(3):537-48.
187. Yamamoto A, Lucas JJ, Hen R. Reversal of neuropathology and motor dysfunction in a conditional model of Huntington's disease. Cell. 2000;101(1):57-66.
188. Harper SQ, Staber PD, He X, Eliason SL, Martins IH, Mao Q, et al. RNA interference improves motor and neuropathological abnormalities in a Huntington's disease mouse model. Proc Natl Acad Sci U S A. 2005;102(16):5820-5.
189. Gu X, Greiner ER, Mishra R, Kodali R, Osmand A, Finkbeiner S, et al. Serines 13 and 16 are critical determinants of full-length human mutant huntingtin induced disease pathogenesis in HD mice. Neuron. 2009;64(6):828-40.
190. McInnis MG. Anticipation: an old idea in new genes. Am J Hum Genet. 1996;59(5):973-9.
191. Parniewski P, Staczek P. Molecular mechanisms of TRS instability. Adv Exp Med Biol. 2002;516:1-25.
192. Harrington JJ, Lieber MR. The characterization of a mammalian DNA structure-specific endonuclease. EMBO J. 1994;13(5):1235-46.
193. Larsen E, Gran C, Saether BE, Seeberg E, Klungland A. Proliferation failure and gamma radiation sensitivity of Fen1 null mutant mice at the blastocyst stage. Mol Cell Biol. 2003;23(15):5346-53.
194. Freudenreich CH, Kantrow SM, Zakian VA. Expansion and length-dependent fragility of CTG repeats in yeast. Science. 1998;279(5352):853-6.
195. Yang J, Freudenreich CH. Haploinsufficiency of yeast FEN1 causes instability of expanded CAG/CTG tracts in a length-dependent manner. Gene. 2007;393(1-2):110-5.
196. van den Broek WJ, Nelen MR, van der Heijden GW, Wansink DG, Wieringa B. Fen1 does not control somatic hypermutability of the (CTG)(n)*(CAG)(n) repeat in a knock-in mouse model for DM1. FEBS Lett. 2006;580(22):5208-14.
197. Spiro C, McMurray CT. Nuclease-deficient FEN-1 blocks Rad51/BRCA1-mediated repair and causes trinucleotide repeat instability. Mol Cell Biol. 2003;23(17):6063-74.
198. Jackson SM, Whitworth AJ, Greene JC, Libby RT, Baccam SL, Pallanck LJ, et al. A SCA7 CAG/CTG repeat expansion is stable in Drosophila melanogaster despite modulation of genomic context and gene dosage. Gene. 2005;347(1):35-41.
199. Otto CJ, Almqvist E, Hayden MR, Andrew SE. The "flap" endonuclease gene FEN1 is excluded as a candidate gene implicated in the CAG repeat expansion underlying Huntington disease. Clin Genet. 2001;59(2):122-7.
200. Lucey BP, Nelson-Rees WA, Hutchins GM. Henrietta Lacks, HeLa cells, and cell culture contamination. Arch Pathol Lab Med. 2009;133(9):1463-7.
201. Hunter JM, Crouse AB, Lesort M, Johnson GV, Detloff PJ. Verification of somatic CAG repeat expansion by pre-PCR fractionation. J Neurosci Methods. 2005;144(1):11-7.
202. Holen T. The ultrastructure of lamellar stack astrocytes. Glia. 2011;59(7):1075-83.
203. Neely JD, Christensen BM, Nielsen S, Agre P. Heterotetrameric composition of aquaporin-4 water channels. Biochemistry. 1999;38(34):11156-63.
204. Frohman MA, Dush MK, Martin GR. Rapid production of full-length cDNAs from rare transcripts: amplification using a single gene-specific oligonucleotide primer. Proc Natl Acad Sci U S A. 1988;85(23):8998-9002.
205. Schmittgen TD, Livak KJ. Analyzing real-time PCR data by the comparative C(T) method. Nat Protoc. 2008;3(6):1101-8.

206. Alwine JC, Kemp DJ, Stark GR. Method for detection of specific RNAs in agarose gels by transfer to diazobenzyloxymethyl-paper and hybridization with DNA probes. Proc Natl Acad Sci U S A. 1977;74(12):5350-4.
207. Towbin H, Staehelin T, Gordon J. Electrophoretic transfer of proteins from polyacrylamide gels to nitrocellulose sheets: procedure and some applications. Proc Natl Acad Sci U S A. 1979;76(9):4350-4.
208. Laemmli UK. Cleavage of structural proteins during the assembly of the head of bacteriophage T4. Nature. 1970;227(5259):680-5.
209. Reynolds JA, Tanford C. Binding of dodecyl sulfate to proteins at high binding ratios. Possible implications for the state of proteins in biological membranes. Proc Natl Acad Sci U S A. 1970;66(3):1002-7.
210. Schagger H, von Jagow G. Blue native electrophoresis for isolation of membrane protein complexes in enzymatically active form. Anal Biochem. 1991;199(2):223-31.
211. Schagger H, Cramer WA, von Jagow G. Analysis of molecular masses and oligomeric states of protein complexes by blue native electrophoresis and isolation of membrane protein complexes by two-dimensional native electrophoresis. Anal Biochem. 1994;217(2):220-30.
212. Heuberger EH, Veenhoff LM, Duurkens RH, Friesen RH, Poolman B. Oligomeric state of membrane transport proteins analyzed with blue native electrophoresis and analytical ultracentrifugation. J Mol Biol. 2002;317(4):591-600.
213. Tajima M, Crane JM, Verkman AS. Aquaporin-4 (AQP4) associations and array dynamics probed by photobleaching and single-molecule analysis of green fluorescent protein-AQP4 chimeras. J Biol Chem. 2010;285(11):8163-70.
214. Wittig I, Braun HP, Schagger H. Blue native PAGE. Nat Protoc. 2006;1(1):418-28.
215. Crick FH. Codon--anticodon pairing: the wobble hypothesis. J Mol Biol. 1966;19(2):548-55.
216. Rash JE, Davidson KG, Kamasawa N, Yasumura T, Kamasawa M, Zhang C, et al. Ultrastructural localization of connexins (Cx36, Cx43, Cx45), glutamate receptors and aquaporin-4 in rodent olfactory mucosa, olfactory nerve and olfactory bulb. J Neurocytol. 2005;34(3-5):307-41.
217. Madrid R, Le Maout S, Barrault MB, Janvier K, Benichou S, Merot J. Polarized trafficking and surface expression of the AQP4 water channel are coordinated by serial and regulated interactions with different clathrin-adaptor complexes. EMBO J. 2001;20(24):7008-21.
218. Crane JM, Van Hoek AN, Skach WR, Verkman AS. Aquaporin-4 dynamics in orthogonal arrays in live cells visualized by quantum dot single particle tracking. Mol Biol Cell. 2008;19(8):3369-78.
219. Westerhout EM, Berkhout B. A systematic analysis of the effect of target RNA structure on RNA interference. Nucleic Acids Res. 2007;35(13):4322-30.
220. Dragatsis I, Levine MS, Zeitlin S. Inactivation of Hdh in the brain and testis results in progressive neurodegeneration and sterility in mice. Nat Genet. 2000;26(3):300-6.
221. Pfister EL, Kennington L, Straubhaar J, Wagh S, Liu W, DiFiglia M, et al. Five siRNAs targeting three SNPs may provide therapy for three-quarters of Huntington's disease patients. Curr Biol. 2009;19(9):774-8.
222. Sorbo JG, Fleckenstein B, Ottersen OP, Holen T. Small-scale purification and mass spectrometry analysis reveal a third aquaporin-4 protein isoform of 36 kDa in rat brain. J Neurosci Methods. 2012;211(1):31-9.
223. Mathiisen TM, Lehre KP, Danbolt NC, Ottersen OP. The perivascular astroglial sheath provides a complete covering of the brain microvessels: an electron microscopic 3D reconstruction. Glia. 2010;58(9):1094-103.
224. Hirt B, Gleiser C, Eckhard A, Mack AF, Muller M, Wolburg H, et al. All functional aquaporin-4 isoforms are expressed in the rat cochlea and contribute to the formation of orthogonal arrays of particles. Neuroscience. 2011;189:79-92.
225. Potokar M, Stenovec M, Jorgacevski J, Holen T, Kreft M, Ottersen OP, et al. Regulation of AQP4 surface expression via vesicle mobility in astrocytes. Glia. 2013;61(6):917-28.
226. Crane JM, Verkman AS. Determinants of aquaporin-4 assembly in orthogonal arrays revealed by live-cell single-molecule fluorescence imaging. J Cell Sci. 2009;122(Pt 6):813-21.
227. Fenton RA, Moeller HB, Zelenina M, Snaebjornsson MT, Holen T, MacAulay N. Differential water permeability and regulation of three aquaporin 4 isoforms. Cell Mol Life Sci. 2010;67(5):829-40.
228. Rossi A, Crane JM, Verkman AS. Aquaporin-4 Mz isoform: brain expression, supramolecular assembly and neuromyelitis optica antibody binding. Glia. 2011;59(7):1056-63.
229. Kozak M. An analysis of 5'-noncoding sequences from 699 vertebrate messenger RNAs. Nucleic Acids Res. 1987;15(20):8125-48.

230. Rossi A, Pisani F, Nicchia GP, Svelto M, Frigeri A. Evidences for a leaky scanning mechanism for the synthesis of the shorter M23 protein isoform of aquaporin-4: implication in orthogonal array formation and neuromyelitis optica antibody interaction. J Biol Chem. 2010;285(7):4562-9.
231. Strecker V, Wumaier Z, Wittig I, Schagger H. Large pore gels to separate mega protein complexes larger than 10 MDa by blue native electrophoresis: isolation of putative respiratory strings or patches. Proteomics. 2010;10(18):3379-87.
232. Jin BJ, Rossi A, Verkman AS. Model of aquaporin-4 supramolecular assembly in orthogonal arrays based on heterotetrameric association of M1-M23 isoforms. Biophys J. 2011;100(12):2936-45.
233. Crane JM, Tajima M, Verkman AS. Live-cell imaging of aquaporin-4 diffusion and interactions in orthogonal arrays of particles. Neuroscience. 2010;168(4):892-902.
234. Nicchia GP, Rossi A, Mola MG, Pisani F, Stigliano C, Basco D, et al. Higher order structure of aquaporin-4. Neuroscience. 2010;168(4):903-14.
235. Crane JM, Verkman AS. Reversible, temperature-dependent supramolecular assembly of aquaporin-4 orthogonal arrays in live cell membranes. Biophys J. 2009;97(11):3010-8.
236. Crane JM, Bennett JL, Verkman AS. Live cell analysis of aquaporin-4 m1/m23 interactions and regulated orthogonal array assembly in glial cells. J Biol Chem. 2009;284(51):35850-60.
237. Assentoft M, Larsen BR, MacAulay N. Regulation and Function of AQP4 in the Central Nervous System. Neurochem Res. 2015;40(12):2615-27.
238. Rutkovskiy A, Stenslokken KO, Mariero LH, Skrbic B, Amiry-Moghaddam M, Hillestad V, et al. Aquaporin-4 in the heart: expression, regulation and functional role in ischemia. Basic Res Cardiol. 2012;107(5):280.
239. Buck L, Axel R. A novel multigene family may encode odorant receptors: a molecular basis for odor recognition. Cell. 1991;65(1):175-87.
240. Solbu TT, Holen T. Aquaporin pathways and mucin secretion of Bowman's glands might protect the olfactory mucosa. Chem Senses. 2012;37(1):35-46.
241. Zhang LJ, Zhao N, Fu Y, Zhang DQ, Wang J, Qin W, et al. Olfactory dysfunction in neuromyelitis optica spectrum disorders. J Neurol. 2015;262(8):1890-8.